

Heinrich-Heine-Universität Düsseldorf

14th of August 2019



Bachelor Thesis

***Characterization of FRET-based
sensors of interfacial macromolecular
crowding***

for obtaining the academic degree

Bachelor of Science

submitted to

Department of Biochemistry

Working group

Synthetic Membrane Systems

by

Samet Kurt

Honorary declaration

I hereby assure, that I have written this bachelor thesis myself and without using any other material, then the cited sources and aids. All posts taken from the sources have been identified as such. The thesis in the same or similar form has not been submitted to any examination body and has not been published.

Düsseldorf, August 9, 2019

Samet Kurt

1st Examiner: Jun.-Prof. Dr. Alexej Kedrov

2nd Examiner: Prof. Dr. Claus A. M. Seidel

Support: Dipl.-Ing. Maryna Löwe

Acknowledgments

I would like to express my appreciation to Jun.-Prof. Dr. Alexej Kedrov for giving me the great opportunity to write my thesis in his workgroup of Synthetic Membrane Systems. I am particularly grateful for the assistance he provided me with and willingness to give his time so generously. This also applies to my supervisor Maryna Löwe, who guided me patiently through the thesis and taught me the theoretical and practical work. A special thanks to you for your advices and critiques. Furthermore, advices given by Athanasios Papadopoulos and Michael Kamel were greatly appreciated.

I really enjoyed and appreciate my time working in this workgroup. You created a relaxed atmosphere in which working was a great pleasure for me. I wish you the best for your academical and personal future.

I also want to thank all the members of the Biochemistry institute for being welcoming and willing to help at all times, as well Prof. Dr. Claus A. M. Seidel for agreeing to be a second examiner

Table of content

| | | |
|----------|--|----|
| 1. | Abstract | 1 |
| 2. | Introduction | 2 |
| 3. | Materials and methods | 4 |
| 3.1. | Materials | 4 |
| 3.1.1. | Buffer..... | 4 |
| 3.1.2. | Constructs of FRET sensor and SecE-SpyCatcher | 6 |
| 3.1.3. | Transformation..... | 6 |
| 3.1.4. | Expression of proteins | 7 |
| 3.1.5. | Purification of proteins..... | 7 |
| 3.1.6. | Cloning of EmrE | 7 |
| 3.1.7. | Liposome manufacturing..... | 8 |
| 3.1.8. | Reconstitution of SecE-SpyCatcher into liposomes | 8 |
| 3.1.9. | Reconstitution of SecE-SpyCatcher into Nanodiscs | 8 |
| 3.1.10. | SDS-PAGE..... | 9 |
| 3.2. | Methods | 9 |
| 3.2.1. | Transformation..... | 9 |
| 3.2.2. | Expression..... | 9 |
| 3.2.2.1. | FRET sensors expression | 9 |
| 3.2.2.2. | SecE-SpyCatcher expression | 11 |
| 3.2.2.3. | MSP expression..... | 11 |
| 3.2.3. | Protein purification | 11 |
| 3.2.3.1. | FRET sensors purification..... | 11 |
| 3.2.3.2. | SecE-SpyCatcher purification | 12 |
| 3.2.3.3. | MSP purification | 13 |
| 3.2.4. | EmrE cloning, expression and purification..... | 13 |
| 3.2.5. | Liposome manufacturing | 15 |
| 3.2.6. | Reconstitution of membrane proteins into synthetic membranes | 16 |
| 3.2.6.1. | Proteoliposomes | 16 |
| 3.2.6.2. | Nanodiscs..... | 16 |
| 3.2.7. | Binding FRET sensor..... | 17 |
| 3.2.8. | Binding streptavidin A1D3 | 17 |
| 3.2.9. | Measurements of emission spectra..... | 17 |
| 4. | Results | 18 |
| 4.1. | Expression and purification of desired proteins | 20 |

| | | |
|--------|--|----|
| 4.1.1. | FRET sensor expression and purification | 20 |
| 4.1.2. | SecE-SpyCatcher (E-SC) expression and purification..... | 26 |
| 4.1.3. | MSP expression and purification | 27 |
| 4.2. | Measurements of emission spectra..... | 28 |
| 4.2.1. | FRET sensors in solution | 28 |
| 4.2.2. | FRET sensor bound to liposomes | 32 |
| 4.2.3. | FRET sensors bound to Nanodiscs | 44 |
| 4.3. | Additional measurements of emission spectra | 48 |
| 4.4. | EmrE-SpyCatcher, EmrE-YFP expression and purification..... | 49 |
| 5. | Discussion..... | 52 |
| 5.1. | Conclusion | 55 |
| 6. | References..... | 56 |
| 7. | List of figures | 57 |
| 8. | List of tables | 59 |
| 9. | List of abbreviations | 60 |

1. Abstract

Cells provide a highly crowded environment in which the excluded volume effect affects equilibria like protein folding and stability. This is barley probed on the cell surface which shows a highly dense packed space with membrane proteins. In this thesis Förster's resonance energy transfer (FRET)-based sensors are presented to investigate crowding on the cell surface. Liposomes and Nanodiscs were used to mimic the cell membrane and crowding agents like polyethylene glycerol (PEG) and streptavidin A1D3 simulated crowding. Whereas synthetic membranes were either cowered by PEG or bound by A1D3. By creating a crowding sensing protein, cellular processes like translocation can be further analyzed and understood. We find that the sensors are affected by crowding in an unbound state but not when bound to the synthetic membrane via SecE-SpyCatcher. Different methods of preparing sensor bound membranes showed first insights to the complexity of probing interfacial macromolecular crowding.

2. Introduction

Cells are highly crowded due to highly abundant cellular macromolecules such as proteins, nucleic acids, ribonucleoproteins, and polysaccharides. Those biological components occupy 5-40 % (corresponds to 80-400 mg/mL) of the cell volume [1]. As a result, the occupied volume is restricted for other molecules and solutes leading to an excluded volume effect. This effect describes the phenomenon that two macromolecules cannot occupy the same space in solution and is increased by steric hindrance or impediment of a macromolecule [2]. In addition, macromolecular crowding can be found on the cell surface, which is highly crowded by membrane proteins. Furthermore, the excluded volume effect is determined by molecular size in which a macromolecule excludes a higher volume than its own size [3]. This dependency is illustrated in figure 1. A molecule smaller than the crowding molecules (molecules indicated as black spheres) can occupy any space (indicated in yellow) in between the crowders (figure 1a). But if a molecule similar in size to macromolecules tries to enter the area, its point of center cannot occupy space in which the surfaces of two molecules would meet (indicated in open circles around macromolecules) (figure 2b).

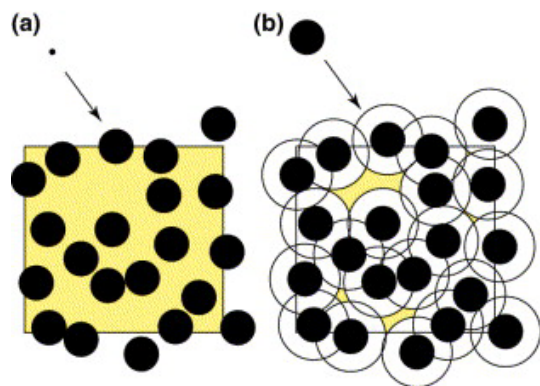


Figure 1: effect of molecular size to excluded volume [3]

Due to the excluded volume effect, macromolecular crowding affects thermodynamic and kinetic processes inside of cells [4]. Furthermore, studies showed that macromolecular crowding have a high impact on conformational stability and structural properties of biological molecules [5]. Those effects can be seen i.e. in protein folding, binding of small molecules, interaction with nucleic acids, enzymatic activity, protein-protein interactions and protein aggregation [2].

In vitro, macromolecular crowding is simulated by synthetic crowding agents like a polysaccharide Ficoll or polyethylene glycol (PEG) [6]. One of approaches to characterize the

crowding employs sensors based on Förster's resonance energy transfer (FRET). The originally designed genetically encoded sensor consists of two fluorophorescent proteins, i.e. mCerulean3 (cyan fluorescent protein, CFP derivate) and mCitrine (yellow fluorescent protein, YFP derivate) connected by a flexible peptide linker [7]. Upon exciting the donor CFP, the acceptor YFP gets excited upon the non-radiant energy transfer from CFP, whereby the distance between acceptor and donor determines the emission intensity of YFP. When introduced into a crowded environment, the sensor adapts a more compressed form leading to a decrease in range between donor and acceptor and an increase of FRET signal [7]. This phenomenon is illustrated in figure 2.

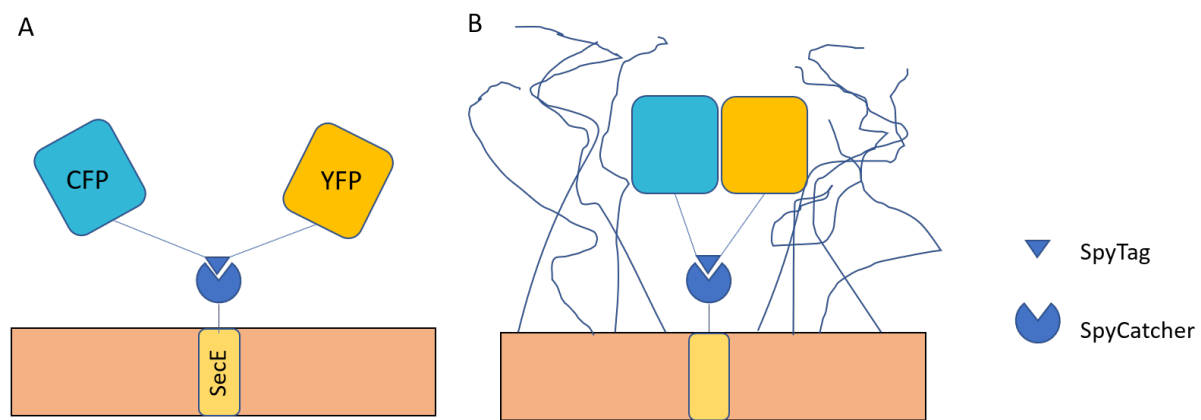


Figure 2: (A) FRET sensor bound to SecE-SpyCatcher on the membrane without crowding (B) FRET sensor bound to SecE-SpyCatcher on the membrane covered with PEG5000

The aim of this study was to express, purify and test the different FRET sensor constructs as well as SecE-SpyCatcher. Tests were performed on the synthetic membranes to probe the efficiency of the FRET sensor in presence of crowder to conclude if the system can be transferred to determine crowding in living cells.

In addition, EmrE-SpyCatcher is cloned, expressed and purified to act as a substitute for SecE-SpyCatcher.

3. Materials and methods

The chemicals used in this thesis are listed below

3.1. Materials

3.1.1. Buffer

| | |
|------------------------------|--|
| 1. Buffer 1 | 40 mM TRIS/HCl (AcrosOrganics) pH 8.0 0.3 M NaCl (Carl Roth) 1 % Triton X-100 (Sigma-Aldrich) |
| 2. Buffer 2 | 40 mM TRIS/HCl pH 8.0 0.3 M NaCl 50 mM cholic acid (Carl Roth) 20 mM imidazole (Sigma-Aldrich) |
| 3. Buffer 3 | 40 mM TRIS/HCl pH 8.0 0.3 M NaCl 20 mM imidazole |
| 4. Capto Core Elution buffer | 30 % isopropyl alcohol (VVR chemicals) in 1 M NaOH (Sigma-Aldrich) |
| 5. Elution buffer Catcher | 50 mM TRIS/HCl pH 7,6 0.1 % DDM (Glycon Bioch.) 300 mM imidazole |
| 6. Elution buffer EmrE | 50 mM TRIS/HCl pH 7.6 150 mM KCl (ChemSolute) 200 µM TCEP (EMD Millipore) 0.1% DDM protease inhibitor cocktail (EDTA free, Roche) |
| 7. Elution buffer FRET | 250 mM imidazole pH 7.6 50 mM NaPi 150 mM KOAc (AppliChem) |
| 8. Elution buffer Nanodiscs | 40 mM TRIS/HCl pH 8.0 0.3 M NaCl 0.4 M imidazole |

| | |
|-----------------------------------|---|
| 9. Liposome buffer | 50 mM TRIS/HCl 150 mM KCl |
| 10. Sodium Phosphate buffer | 137.8 g/L disodium phosphate (Carl-Roth) pH 7.4 |
| | 31.2 g/L monosodium phosphate (AppliChem) |
| 11. Resuspension buffer Catcher50 | mM TRIS/HCl pH 7.4 100 mM KCl protease inhibitor cocktail 5 % glycerol (Sigma-Aldrich) |
| 12. Resuspension buffer FRET | 10 mM sodium phosphate buffer pH 7.6 100 mM KOAc 0.1 mM PMSF protease inhibitor cocktail 5 % Glycerol |
| 13. Resuspension buffer Nanodiscs | 20 mM sodium phosphate buffer pH 8.0 protease inhibitor cocktail |
| 14. SEC buffer Catcher | 50 mM TRIS/HCl pH 7.6 100 mM KCL 0.05 % DDM protease inhibitor cocktail |
| 15. SEC buffer FRET | 10 mM sodium phosphate buffer pH 7.6 |
| 16. SEC buffer Nanodiscs | 20 mM TRIS/HCl pH 7.4 0.1 M NaCl 0.5 mM EDTA (AppliChem) |
| 17. SEC buffer liposomes | 50 mM TRIS/HCl pH 7.6 100 mM KCl |
| 18. Solubilization buffer | 50 mM TRIS/HCl pH 7.6 100 mM KCl 200 µM TCEP 1% DDM |

| | |
|-------------------------|--|
| 19. Wash buffer Catcher | 50 mM Tris/HCl pH 7.6 100 mM KCl 10 mM imidazole 0.1 % DDM |
| 20. Wash buffer EmrE | 50 mM TRIS/HCl pH 7.6 150 mM KCl 200 µM TCEP 0.1% DDM 10 mM imidazole protease inhibitor cocktail |
| 21. Wash buffer FRET | 20 mM imidazole pH 7.6 50 mM NaPi 150 mM KOAc |

3.1.2. Constructs of FRET sensor and SecE-SpyCatcher

The different constructs for FRET sensors and SecE-SpyCatcher are listed below.

Table 1: FRET sensor and SecE-SpyCatcher constructs used in this thesis

| construct | |
|----------------------|--|
| FRET 107 | CFP-(GSG) ₆ -SpyTag-(GSG) ₆ -YFP |
| FRET 148 | CFP-(GSG) ₆ -Helix ³² -(GSG) ₄ -SpyTag-(GSG) ₄ -Helix ³² -(GSG) ₆ -YFP |
| FRET 155 | CFP-(GSG) ₆ -Helix ¹⁵ -(GSG) ₂ -SpyTag-(GSG) ₂ -Helix ¹⁵ -(GSG) ₆ -YFP |
| SecE-SpyCatcher-126 | SecE-(GSG) ₆ -Helix ³² -(GSG) ₆ -SpyCatcher |
| SecE-SpyCatcher-126A | SecE-(GSG) ₆ -Helix ¹⁵ -(GSG) ₆ -SpyCatcher |
| SecE-SpyCatcher-126B | SecE-(GSG) ₆ -SpyCatcher |

3.1.3. Transformation

1. *Escherichia coli* (*E. coli*) C41(DE3) cells
2. Plasmids
3. LB Medium (Carl Roth)

| |
|---------------------------------|
| 10 g/l Tryptone (Carl-Roth) |
| 10 g/l NaCl |
| 5 g/l yeast Extract (Carl-Roth) |

4. LB-Agar plates supplemented with 100 µg/ml ampicillin (Applichem)

3.1.4. Expression of proteins

1. LB Medium (Carl Roth)
2. TB Medium 12 g/L tryptone
 24 g/L yeast extract
 0.5 % glycerol
TB salt 23.1 g/L monopotassium phosphate (Sigma-Aldrich)
 164.32 g/L dipotassium phosphate (Carl-Roth)
3. 100 mg/mL Ampicillin
4. 50 mg/mL Kanamycin (Carl Roth)
5. *E. coli* cells transformed with plasmids
6. 1M IPTG (Carbolution)

3.1.5. Purification of proteins

1. Ni-NTA agarose beads (Qiagen)
2. Glass beads (100 µm, Bio-Budget)
3. 5-10 mM imidazole
4. Superdex 200 Increase 10/300 GL (GE Healthcare)
5. Capto Core 400 (GE Healthcare)
6. Buffer Exchange column (PD SpinTrap, GE Healthcare)

3.1.6. Cloning of EmrE

1. PCR clean up kit (Macherey-Nagel)
2. Plasmid-isolations kit (Macherey-Nagel)
3. KOD-polymerase kit (NEB)
4. Gibson Assembly kit (NEB)
5. DpnI (NEB)
6. LB-Agar plates supplemented with ampicillin
7. Mix2Seq Kit (eurofins)
8. Primer

3.1.7. Liposome manufacturing

All lipids used were purchased by Avanti Polar Lipids Inc. / Otto Nordwald GmbH and are listed below. Liposomes were manufactured with an Extruder (Avanti Polar lipids) using Filter support (Avanti Polar Lipids Inc.) and membranes with a pore size of 800 nm and 200 nm (Avanti Polar Lipids Inc.).

1. 25 g/L 1,2-dioleoyl-sn-glycero-3-phosphoglycerol (DOPG)
2. 25 g/L 1,2-dioleoyl-sn-glycero-3-phosphocholine (DOPC)
3. 25 g/L 1,2-dioleoyl-sn-glycero-3-phosphoethanolamine (DOPE)
4. 10 g/L 1,2-dioleoyl-sn-glycero-3-phosphoethanolamine-N-[methoxy(polyethylene glycol)-5000] (DOPE-PEG5000)
5. 10 g/L 1,2-dioleoyl-sn-glycero-3-phosphoethanolamine-N-(biotinyl) sodium salt (DOPE-Biotin)
6. 10 g/L 1,2-dierucoyl-sn-glycero-3-phosphocholine (22:1 PC)

3.1.8. Reconstitution of SecE-SpyCatcher into liposomes

1. 5 mM liposomes, 200 nm extruded
2. Purified SecE-SpyCatcher
3. 10 % DDM
4. 70 mg Bio-Beads SM2 (Bio-Rad Laboratories)

3.1.9. Reconstitution of SecE-SpyCatcher into Nanodiscs

1. 5 mM liposomes, 200 nm extruded
2. Purified SecE-SpyCatcher
3. Purified MSP
4. 10 % DDM
5. 10 % Triton-X
6. 70 mg Bio-Beads SM2

3.1.10. SDS-PAGE

1. 15% sodium dodecyl sulfate polyacrylamide gels for electrophoresis (SDS-PAGE), prepared following Cold Spring Harbor protocols [8]
2. PageRuler Prestained protein ladder (Thermo Fisher Scientific)
3. Sample buffer

| |
|-------------------------------|
| 250 mM TRIS/HCl pH 6.8 |
| 10 % SDS |
| 30 % glycerol |
| 0,5 M DTT |
| 0.05 % (w/v) brom-phenol-blue |
4. Quick Coomassie Stain (Serva)

3.2. Methods

3.2.1. Transformation

All cell transformations with plasmids were carried out as described below. 0.3 µL of plasmid (concentration 50-100 ng/µL) were added to C41(DE3) cells and incubated on ice for 3 min. After a 1 min heat shock at 42 °C, cells were transferred on ice again for 2 min. 500 µL LB-medium was added and incubated for 30 min (37 °C, 150 rpm). Then, 100 µL of cell suspension was plated out on an agar plate supplemented with 100 µg/ml ampicillin.

3.2.2. Expression

3.2.2.1. FRET sensors expression

FRET 155 test expression

Colonies were picked from the plate and transferred to two overnight cultures, one with 20 mL LB- and one with 100 LB-medium supplemented with 100 µg/mL ampicillin. 100 mL culture was incubated for 4 hours (37 °C), induced with 0.1 mM IPTG and incubated at 25 °C overnight. 20 mL preparation was incubated overnight at 37 °C. After incubation, it was split up into six flasks each containing 200 mL LB-medium supplemented with ampicillin. Three bottles each were incubated at 30 °C and 37 °C. Cells were grown until OD₆₀₀ of 0.6 was reached. The

protein expression was induced with either 0.1 mM or 0.5 mM IPTG. For each temperature one IPTG-free sample was also examined.

Cells were then collected by centrifugation at 5000 g (7 min at 4 °C). The supernatant was discarded and each pellet was resuspended in 2 mL Resuspension buffer FRET (see materials 3.1.1). Samples were then flash-frozen in liquid nitrogen and stored at -80 °C until further processing.

800 µL of samples before induction and cell harvesting were lysed by B-PER. For this, B-PER was mixed with 100 µg/mL lysozyme, 40 µg/mL DNase and complete protease inhibitor cocktail. Cells were then centrifuged for 2 min at 14,860 g and resuspended in B-PER. The resuspension volume corresponds to the OD using the following formula:

$$\text{Resuspension volume} = \frac{\text{OD}}{9,625}$$

Samples were then incubated at room temperature for 15 min and analyzed by SDS-PAGE. All following lyses by B-PER were carried out the same way.

FRET 107, 148, 155 large scale expression

One colony was picked out of each plate and transferred to an overnight culture containing 20 mL LB-amp with 1 % glucose and 100 µg/ml ampicillin. Cells were incubated at 30 °C and 180 rpm overnight. 3 flasks, each containing 1 L TB-medium supplemented with ampicillin, were inoculated with the overnight cultures. TB-medium was prepared in a ratio of 1:10 (w/w TB-salt:TB-medium). Cells were grown at 30 °C and 170 rpm until an OD of 0.6 was reached. Cells were then induced with 0.1 mM IPTG and incubated overnight at 25 °C. Cells were harvest by centrifugation (SLC-6000 rotor, Thermo Fisher Scientific) at 6000 g for 12 min and resuspended in 15 mL Resuspension buffer FRET (see materials 3.1.1). Samples were then frozen in liquid nitrogen and stored (-80 °C) for further processing. In a separate experiment, expression of FRET 155 construct in TB and LB media was compared, following the same protocol.

Samples of each flask were taken before induction and before cell harvesting, lysed by B-PER and analyzed via SDS-PAGE.

3.2.2.2. SecE-SpyCatcher expression

Three 20 mL overnight cultures (LB-medium) supplemented with 100 µg/mL and containing cells with SecE-SpyCatcher-126, 126A and126B plasmids were transferred to flasks with 1 L LB-medium supplemented with 100 µg/mL ampicillin. Growth and expression with 0.1 mM IPTG were taken place at 37 °C and 180 rpm. Cells were harvest by centrifugation (SLC-6000 rotor) at 6000 g for 12 min and resuspended in 15 mL Resuspension buffer Catcher (see materials 3.1.1). Samples were then frozen in liquid nitrogen and stored (-80 °C) until further processing.

Samples of each flask were taken before induction and before cell harvesting, lysed by B-PER and analyzed via SDS-PAGE.

3.2.2.3. MSP expression

Cells containing MSPE3D1- and MSP2N2-encoding plasmids were grown in 2 L TB-medium supplemented with 50 µL/L kanamycin at 37 °C and 180 rpm until an OD of 0.5 was reached. The protein induction was induced with 1 mM IPTG. Cells were harvested by centrifugation (SLC-6000 rotor) at 6000 g for 12 min and resuspended in 15 mL Resuspension buffer Nanodiscs (see materials 3.1.1). Samples were then frozen in liquid nitrogen and stored (-80 °C) until further processing.

Samples of each flask were taken before induction and before cell harvesting, lysed by B-PER and analyzed via SDS-PAGE.

3.2.3. Protein purification

3.2.3.1. FRET sensors purification

FRET 155 test purification

200 µL Ni-NTA agarose beads was used for each sample. Columns with beads were centrifuged at 1000 rpm for 30 sec in Eppendorf table-top centrifuge. 0.5 mL water was added and centrifuged again. Columns were then washed twice with 0.5 mL Wash buffer FRET (see materials 3.1.1) each and centrifuged. 800 µL of lysed cells (with B-PER) were centrifuged at

14000 rpm (20.000 g) for 2 min to remove cell debris. The supernatants were then added to the columns and incubated for 15 min. Flow-through was collected by centrifugation and beads were then washed twice with 800 µL Wash buffer FRET. Elution was carried out in two steps, each with 100 µL Elution buffer FRET (see materials 3.1.1) after 3 min incubation. Sample at 25 °C was further purified via SEC. For SEC, Superdex 200 Increase 10/300 GL column was equilibrated at a flow rate of 0.6 mL/min with 25 mL buffer and then loaded with the sample. Elution was carried out with 25 mL of the same buffer using the same flow rate. After, 0.5 mL fractions were collected and analyzed by SDS-PAGE. Those settings were used for all size exclusions.

FRET 107, 148, 155 large scale purification

1.5 mL Ni-NTA agarose beads was washed for each preparation and equilibrated with Wash buffer FRET. Cell lysate (disrupted by Microfluidizer, M-110P-Microfluidics) was centrifuged (SS-34 rotor, Thermo Fisher Scientific) at 12.000 rpm for 20 min to remove the cell debris. The supernatant was loaded on the column and incubated for 60 min. The flow-through was collected and beads were washed three times each with 18 mL Wash buffer FRET. FRET sensors were then eluted twice each with 2 mL Elution buffer FRET. First elution was further analyzed by SEC.

3.2.3.2. SecE-SpyCatcher purification

Cells were disrupted by Microfluidizer and centrifuged (SS-34 rotor) at 5000xg for 15 min to remove the cell debris. In order to gather membranes, the supernatant was centrifuged (Ti70 rotor, Beckman Coulter) at 40,000xg for 50 min. The pellet containing membranes was resuspended in Resuspension buffer Catcher (see materials 3.1.1). 400 µL membranes were then solubilized in Solubilization buffer (see materials 3.1.1) and incubated for 60 min. After 10 min centrifugation at 14,680xg, 5 mM imidazole was added and the lysate was purified via Ni-NTA. For this 0.5 mL Ni-NTA-agarose beads was used. Beads were washed and equilibrated with Wash buffer Catcher (see materials 3.1.1). Solubilized membranes were added and incubated for 60 min. The samples were then washed three times with 5 mL Wash buffer Catcher and eluted with 1 mL Elution buffer Catcher (see materials 3.1.1). Elutions were subject to buffer exchange using SEC buffer catcher (see materials 3.1.1).

3.2.3.3. MSP purification

1 % Triton X-100 was added to harvested cells before cell disruption. Disrupted cells (by Microfluidizer) were then centrifuged (Ti45 rotor, Beckman Coulter) at 16100 rpm for 30 min. Next the lysate was purified via Ni-NTA using 0.75 mL Ni-NTA-agarose beads as described in FRET large scale purification. Elution took place in several steps each with 1 ml Elution buffer Nanodiscs. Eluted samples were combined and concentrated to 2 mL. MSPE3D1 was further subject to buffer exchange using SEC buffer Nanodiscs (see materials 3.1.1).

3.2.4. EmrE cloning, expression and purification

Cloning

Templates for EmrE and SpyCatcher were provided by Alexej Kedrov. EmrE insert was prepared via a 2 step PCR. For the first step KOD-Polymerase kit was used. 0,5 µL KOD-polymerase was added to a mix of 12,5 µL Xtreme buffer, 6 µL water, 5 µL dNTPs, 1,5 µL template (*E. coli* DH5α genomic DNA) and 0,2 µL of each primer (EmrE_gene_FW and EmrE_gene_Re). Also, a negative control without primers was prepared. Both samples were placed in a thermal cycler which was run for 30 cycles with the settings listed in table 2.

Table 2: PCR settings for first step of EmrE insert preparation

| | | | |
|--------|-------|--------|----------------------------------|
| Step 1 | 98 °C | 30 sec | |
| Step 2 | 62 °C | 30 sec | 0,3 °C decrease after each cycle |
| Step 3 | 68 °C | 25 sec | |

The product was further used as the new template for the second step of insert preparation to introduce overhangs for Gibson assembly. Samples for PCR were prepared as described before. For this step pKAD163_EmrE_A_Fw and pKAD163_EmrE_B_Re were used as primers. Settings for the PCR are listed in table 3.

Table 3: PCR settings for second step of EmrE insert preparation

| | | | |
|--------|-------|--------|----------------------------------|
| step 1 | 98 °C | 30 sec | |
| step 2 | 62 °C | 30 sec | 0,3 °C decrease after each cycle |
| step 3 | 68 °C | 50 sec | |

The backbone vector containing the SpyCatcher gene was multiplied in PCR with KOD-Polymerase as describes before for EmrE. Primers pKAD163_EmrE_A_Re and pKAD163_EmrE_B_Fw were used together with the template for SpyCatcher. The PCR was started with the settings listed in table 4.

Table 4: PCR setting for SpyCatcher vector preparation

| | | | |
|--------|-------|----------|----------------------------------|
| Step 1 | 98 °C | 30 sec | |
| Step 2 | 70 °C | 30 sec | 0,3 °C decrease after each cycle |
| Step 3 | 68 °C | 3:30 min | |

PCR products were then cleaned by PCR-Clean-Up kit. Template DNA were removed by adding 2 µL CutSmart buffer and DpnI to 17 µL PCR product and incubating for 30 min at 37 °C. Both samples were again cleaned with PCR-Clean-Up kit. The vector and insert with overhanging ends were merged via Gibson-Assembly. For this, three preparations with different ratios of insert and vector were created (table 5).

Table 5: Composition of preparations for Gibson-Assembly

| | Preparation 1 (negative) | Preparation 2 | Preparation 3 |
|-----------------------|--------------------------|---------------|---------------|
| Master Mix | 5 µL | 5 µL | 5 µL |
| Vector (SpyCatcher) | 3 µL | 3 µL | 3 µL |
| Insert (EmrE) | 0 µL | 0.5 µL | 1.5 µL |
| Water | 2 µL | 1.5 µL | 0.5 µL |
| Ratio (insert:vector) | 0:1 | 1:6 | 1:3 |

Samples were incubated at 50 °C for 20 min and then transformed into 100 µL C41(DE3) cells as describes in methods 3.2.1, using 10 µL product of the Gibson-Assembly instead of 0.3 µL plasmid. Transformed cells were then plated on LB-agar-plates supplemented with 100 µg/ml ampicillin leaving them for incubation at 37 °C overnight. 6 colonies of each plate were picked and transferred to 2,5 mL LB-medium supplemented with ampicillin. These were again incubated at 37 °C overnight. Plasmid-isolation-kit and was used for each sample. Sequence was checked by using Mix2Seq kit and confirmed by Eurofins genomics. The successfully cloned plasmid was then transferred into C41(DE3) cells and cells were plated on LB-agar-plates supplemented with 100 µg/mL ampicillin.

Furthermore EmrE-YFP plasmid was prepared by my supervisor Maryna Löwe with N-terminal EmrE and C-terminal YFP.

Expression and purification

EmrE-SpyCatcher and EmrE-YFP cells were grown and expressed twice. First, EmrE-SpyCatcher was expressed as described in the protocol for SecE-SpyCatcher purification (see methods 3.2.2). EmrE-YFP was then expressed in 100 mL LB-medium supplemented with 100 µg/mL ampicillin at 30 °C and 37 °C. Both, EmrE-SpyCatcher and -YFP, were then again expressed as at 30 °C.

For the first expression of EmrE-SpyCatcher, harvested cells were processed up to the solubilization step. Next, 400 µL membranes were solubilized with Solubilization buffer and incubated for 40 min at 4 °C on a rolling bench. After, 5 mM imidazole was added, and the sample was split into three samples, each 1 mL. Each sample was then subject to Ni-NTA purification using Wash buffer EmrE (see materials 3.1.1) containing 10 mM, 20 mM or 30 mM imidazole. 50 µL Ni-NTA-agarose beads was used for each preparation. Elutions were further analyzed by SDS-PAGE.

Harvested cells of EmrE-YFP of the first expression were lysed using two different methods. For the first method, cells of 30 °C expression were centrifuged at 5000xg for 20 min and resuspended in 2 mL Resuspension buffer Catcher. 0.5 mL glass beads were added and the sample was vortexed for 5 min to lyse the cells. Next, the sample was centrifuged at 14,000xg for 5 sec, removing the glass beads. The supernatant containing lysed cells was centrifuged at 14,000xg for 1 min to remove cell debris. Again, supernatant containing membranes was centrifuged at 14,860xg for 20 min and analyzed by SDS-PAGE. For the next method, harvested cells of 37 °C expression were lysed in 2 mL B-PER. After centrifugation at 14,860xg for 10 min, the supernatant was analyzed by SDS-PAGE.

After the second expression of EmrE-SpyCatcher and EmrE-YFP, resuspended cells were disrupted by Microfluidizer. Samples were centrifuged (SS-34 rotor) at 5000xg for 15 min to remove cell debris. The supernatant was centrifuged (Ti45 rotor) at 40,000xg for 50 min in order to pellet the membranes. Those were resuspended in Resuspension buffer Catcher and analyzed by SDS-PAGE.

3.2.5. Liposome manufacturing

Chosen lipids solubilized in chloroform were mixed in desired concentration. Chloroform was evaporated using a rotary evaporator at 35 °C, 150 rpm and 350 mbar for approx. 40 min.

Resulting lipid film was resuspended in Liposome buffer (see materials 3.1.1) to reach an end concentration of 5 mM lipids. Resuspended liposomes were extruded first to 800 nm, then to 200 nm forming homogenous liposomes. Compositions of liposomes used for measurements in this thesis are listed in table 6.

Table 6: Lipid composition of liposomes used in this thesis

| Liposome composition | Fraction (mol %) |
|----------------------------|------------------|
| PC:DOPG:DOPE | 10:80:10 |
| PC:DOPG:DOPE-PEG5000 | 10:80:10 |
| DOPC:DOPG:DOPE:DOPE-Biotin | 60:30:9:1 |
| DOPC:DOPG:DOPE:DOPE-Biotin | 60:30:5:5 |
| DOPC:DOPG:DOPE-Biotin | 60:30:10 |
| DOPC:DOPG:DOPE | 60:30:10 |
| DOPC:DOPG:DOPE-PEG5000 | 60:30:10 |

3.2.6. Reconstitution of membrane proteins into synthetic membranes

3.2.6.1. Proteoliposomes

Membrane proteins (SecE-SpyCatcher derivatives) were reconstituted at a protein:lipid molar ratio of 1:3000, and the detergent was removed with Bio-Beads SM2 sorbent (Bio-Rad). Bio-Beads were washed beforehand twice with methanol, twice with ethanol and 3 times with water. For reconstitution, 200 µL of liposomes were destabilized by 0.3 % DDM and incubated for 15 min at 30 °C. 300 µL of Liposome buffer containing 0.05 % DDM and SecE-SpyCatcher was added afterwards. The sample was incubated for 20 min on ice. Then, 70 mg Bio-Beads SM2 sorbent were added and the mix was rolled on a rolling bench overnight at 4 °C. The next day, suspension was pipetted and centrifuged (AT3-rotor, Thermo Fischer Scientific) at 60,000xg for 30 min if necessary. Pelleted proteoliposomes were then resuspended in Liposome buffer with the desired volume.

3.2.6.2. Nanodiscs

A molar ratio of 2:10:500 and 2:10:800 (SecE-SpyCatcher : MSP : lipid) was used for MSP1E3D1 and MSP2N2, respectively. 100 µL of liposomes were destabilized with 0.5 % Triton X-100 and

incubated for 15 min at 30 °C. Liposome buffer containing 0.05 % DDM and SecE-SpyCatcher were added together. Afterwards, lipids and MSP of choice was added. Preparation was filled up to 500 µL with Liposomes buffer and was incubated for 20 min on ice. Then, 70 mg Bio Beads were added and the mix was rolled on a rolling bench overnight at 4 °C. The next day, the supernatant was pipetted and centrifuged at 14,860 g for 15 min. The supernatant was used for further measurements.

3.2.7. Binding FRET sensor

FRET sensors were bound to SecE-SpyCatcher. For this, three methods were used.

1. FRET was added to proteoliposomes or Nanodiscs in excess to SecE-SpyCatcher. The sample was then incubated for 1 hours and 200 µL was purified by SEC column using SEC buffer liposomes.
2. FRET was added in a 1:5 (FRET sensor : SecE-SpyCatcher) mol ratio to proteoliposomes and incubated for 4 hours.
3. FRET was added in excess to SecE-SpyCatcher. The sample was incubated for 3 h and fractionated via SEC using SEC buffer Catcher. Purified fractions containing the protein complex were collected, pooled and used for further reconstitution into proteoliposomes.

3.2.8. Binding streptavidin A1D3

A1D3 was added to FRET-bound proteoliposomes or Nanodiscs to bind biotin. For this, we assumed that 50 % biotinylated lipids were facing inwards and couldn't be accessed by A1D3. The amount for A1D3 addition was then calculated equimolar to biotin facing outwards.

3.2.9. Measurements of emission spectra

60 µL of sample was pipetted to a 3x3 mm quartz cuvette (High Precision Cell). Fluorescence intensity was measured by spectrofluorometer (Fluorolog-3 HORIBA Scientific). FRET donor was excited at 420 nm. The emission for both the FRET donor and acceptor was detected from 430 nm to 620 nm with an increment of 1 nm.

4. Results

In this study the SpyTag/SpyCatcher system [9] was used to anchor FRET sensors to the surface of synthetic membranes with the aim to characterize the interfacial macromolecular crowding. This anchoring system allows proteins fused with the SpyTag peptide and the SpyCatcher protein to form spontaneously a covalent isopeptide bond between residues [9]. SpyTag has been introduced into the FRET sensor, and the SpyCatcher has been fused with transmembrane helices 1 and 2 of *Escherichia coli* SecE, a subunit of SecYEG translocon. With this membrane-anchored complex, crowding can be potentially detected in cellular membranes or liposomes or Nanodiscs, which mimic the membrane of living cells. Liposomes are phospholipid spheres with a bilayered membrane structure [10]. Nanodiscs on the other hand are a disc-shaped lipid bilayer of phospholipids held together by a belt formation of two membrane scaffold proteins (MSP) and are used for study of membrane proteins. Those MSPs are modified versions of apolipoprotein A1, which have a role in the lipid metabolism [11].

Furthermore, three versions of FRET sensors and SecE-SpyCatcher were used. FRET 107 consists of CFP-(GSG)₆-SpyTag-(GSG)₆-YFP, while GSG describes the sequence of the glycine-serine-glycine linker repeats. When CFP and YFP are connected solely by this flexible linker, the sensor manifests a high FRET signal in its uncompressed form, so CFP and YFP appear in a close vicinity [7]. In FRET 148 two α -helices are added between the fluorophores and SpyTag, with shorter linker between the helix and SpyTag (CFP-(GSG)₆-Helix³²-(GSG)₄-SpyTag-(GSG)₄-Helix³²-(GSG)₆-YFP). Adding helices to the construct results in a repulsion of the fluorophores. In FRET 155 those helices are half in size with even shorter linker between the helix and SpyTag. With the CFP-(GSG)₆-Helix¹⁵-(GSG)₂-SpyTag-(GSG)₂-Helix¹⁵-(GSG)₆-YFP sequence. SecE-SpyCatcher 126 consists of SecE-(GSG)₆-Helix³²-(GSG)₆-SpyCatcher. In SecE-SpyCatcher 126A the α -helix is halved, and in SecE-SpyCatcher 126B the helix is removed. The latter one allows the sensor binding being closer to the surface leading to more natural environment. Those variants can be seen in figure 3.

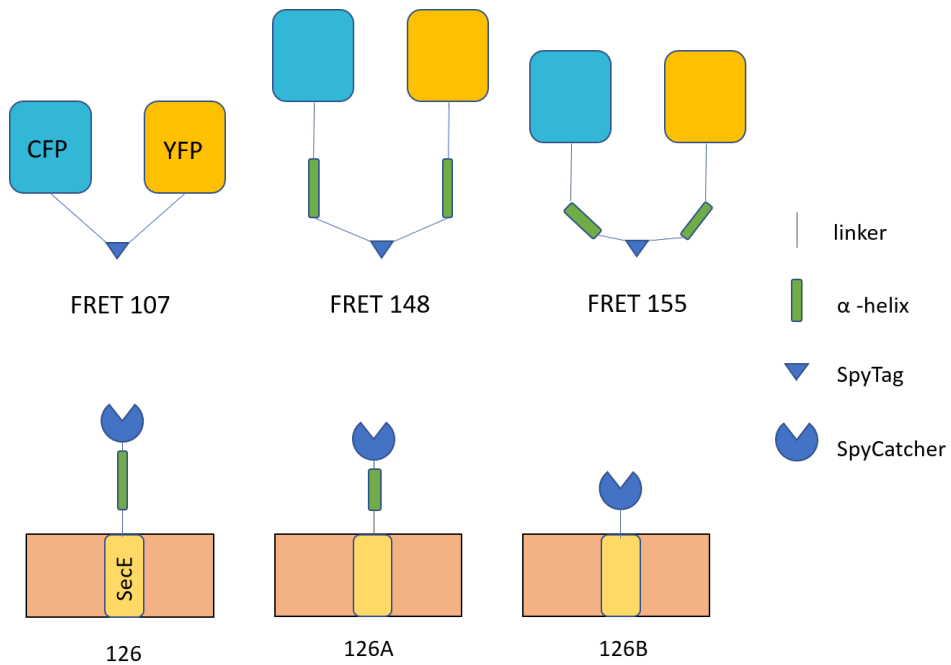


Figure 3: different versions of FRET sensors and SecE-SpyCatcher

Macromolecular crowding in solution was tested with PEG4000 and Ficoll PM70 for unbound FRET sensors. For simulating crowding on the cell surface, PEG5000 covered liposomes and Nanodiscs were used. This was also tested by using streptavidin that can bind to biotinylated liposomes/Nanodiscs and may act as a proteinaceous crowding agent. Streptavidin is a tetramer consisting of four identical monomers, and each of those can bind biotin. To hinder all four monomers of binding, the monovalent mutant A1D3 was used which consists of the dead monomers (D3) and one functional biotin binding monomer (A1) [12].

First, an expression test with FRET sensor were performed to achieve correctly folded proteins. FRET sensors, SecE-SpyCatcher and MSP were then expressed and purified for measurement preparation. After testing the sensor performance, we tried to find an appropriate way to anchor sensors and detect macromolecular crowding.

4.1. Expression and purification of proteins

4.1.1. FRET sensor expression and purification

FRET 155 test expression and purification

FRET 155 was expressed under 7 conditions. Preparation 1 (30°C , 0 mM IPTG) showed the highest growth with an OD_{600} of 1.14. This might be since a baffled flask was used for this sample. Two data sets of samples took before induction and before cell harvesting were analyzed by SDS-PAGE (figure 4). One set was boiled at 95°C for 5 min in order to see the protein in its native conformation. Several bands with fluorescence can be seen in figure 4A. This might be due to different conformations of FRET 155 or cleaved fluorophores, which aren't visible in the boiled version. The highest fluorescence intensity before cell harvesting was seen for preparation 7 (25°C , 0.1 IPTG), i.e. after the overnight expression.

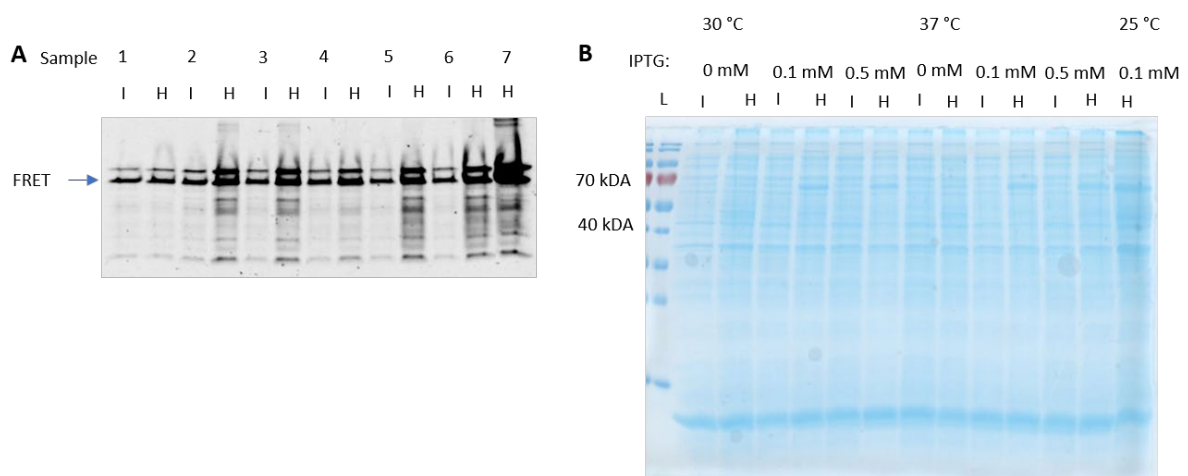


Figure 4: 15 % SDS-PAGE of lysed cells before induction and before cell harvesting for preparations 1-7 of FRET 107. L=protein ladder, I= sample before Induction, H= before cell harvesting (A) fluorescence image at 460 nm of nonboiled samples (B) colorimetric image of Coomassie-stained boiled samples

Cells resuspended in Resuspension Buffer FRET were lysed by B-PER and then purified by Ni-NTA. Preparation 7 was further purified by SEC. Ni-NTA purification (figure 5) for all preparations showed a successful elution of the protein. The highest protein absorbance was measured for preparation 7 which still fluoresced in the flow-through. Preparations 2, 3 and 7

had the highest fluorescence intensity in the flow-through showing an overload of protein. Using more Ni-NTA-agarose beads would have led to a higher yield.

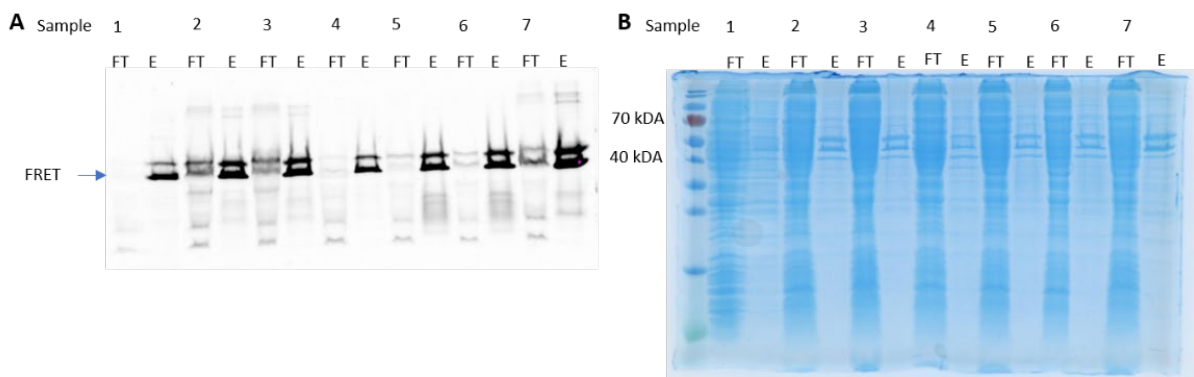


Figure 5: 15% SDS-PAGE of IMAC purification of FRET 107. (A) fluorescence image at 460 nm (B) colorimetric image of Coomassie-stained unboiled samples. FT= flow-through, E= Elution.

SEC (figure 6) showed two peaks at \approx 9mL and \approx 12mL. Fractions 12.5 mL – 14 mL from SEC displayed the purified protein at \approx 50 kDa. Predicted molecular mass of the sensor is at approx. 50-55 kDa. Those fractions were pooled and used for further measurements.

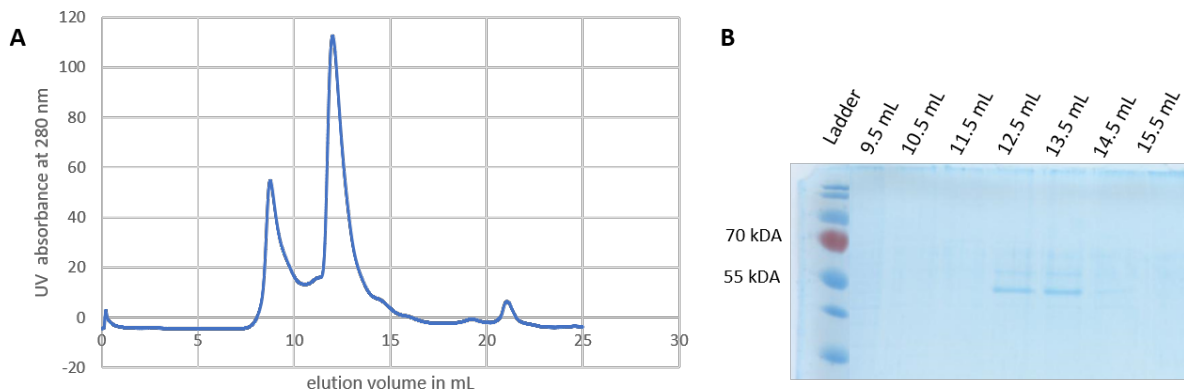


Figure 6: (A) chromatogram of SEC for preparation 7 (B) colorimetric image of 15 % SDS-PAGE with Coomassie-stained SEC elution fractions

Furthermore, the absorbance spectrum (figure 7) of preparation 7 was probed by NanoDrop Spectrophotometer ND-1000 (Peqlab Biotechnologie GmbH) from 300-600 nm. The sample showed characteristic peaks attributed to the donor mCerulean3 (cyan fluorescence protein, CFP) around 433 nm and the acceptor mCitrine (yellow fluorescence protein, YFP) at appx. 516 nm. The absorbance maximum for CFP have been too low thus suggesting incorrect folding of the CFP domain, probably due to longer maturation times. The fluorescence intensity is dependent to extinction coefficient x quantum yield. CFP's ($33,000 \text{ M}^{-1} \text{ cm}^{-1} \times 0.42$) is 3 times

lower than YFP's ($69,000 \text{ M}^{-1} \text{ cm}^{-1} \times 0.72$) thus the fluorescence intensity will be appx. 3 times lower [13].

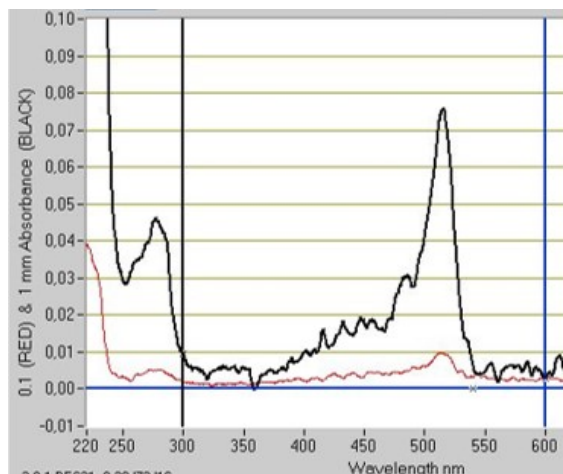


Figure 7: Absorbance spectrum for FRET 155 test (preparation 7)

FRET 107, 148, 155 large scale expression and purification

FRET sensors were expressed overnight at 25 °C to provide enough time for protein maturation. Each cell culture grew similar with an OD_{600} of ≈ 0.6 . Samples before induction and cell harvesting were lysed by B-PER and analyzed by SDS-PAGE (figure 8). Expression succeeded due to the high fluorescence intensity in the samples before cell harvesting.

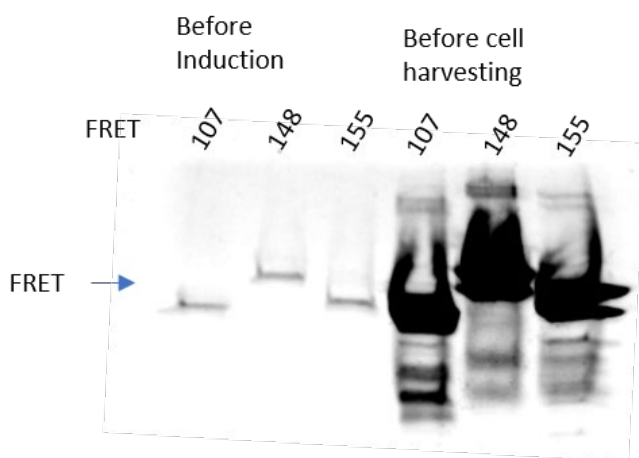


Figure 8: Colorimetric image of 15 % SDS-PAGE with lysed cells before induction and before cell harvesting for FRET 107, 148, 155

Ni-NTA purification for each sensor, visible at \approx 55 kDa, showed a loss of sensor after each washing step (figure 9,10,11). Still, a high amount of FRET sensor was found in the elution fraction.

SEC has displayed 2 peaks for each sensor, one at \approx 9 mL (void volume, aggregated material) and one at around 12.5 – 13 mL. Due to the difference in size and, likely, the conformation, the sensors eluted at slightly different volumes. The gels showed several bands after SEC which might be due conformational changes and poor denaturation of fluorescent proteins in SDS. For FRET 107 fractions 13.5-15 mL were pooled.

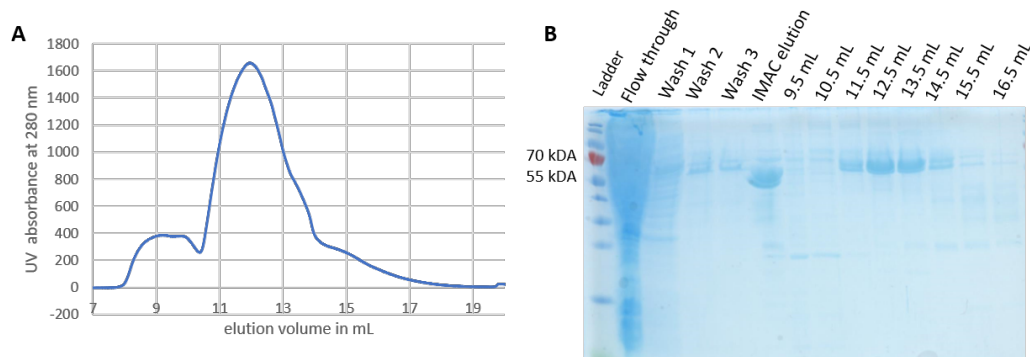


Figure 9: (A) chromatogram of SEC for FRET 107 (B) colorimetric image of 15 % SDS-PAGE with Coomassie-stained Ni-NTA purification and SEC elution fractions of FRET 107

FRET 148 displayed a peak at \approx 13 mL in the chromatogram (figure 10A) with fractions 12.5-14 mL containing the highest protein concentration. Those were pooled.

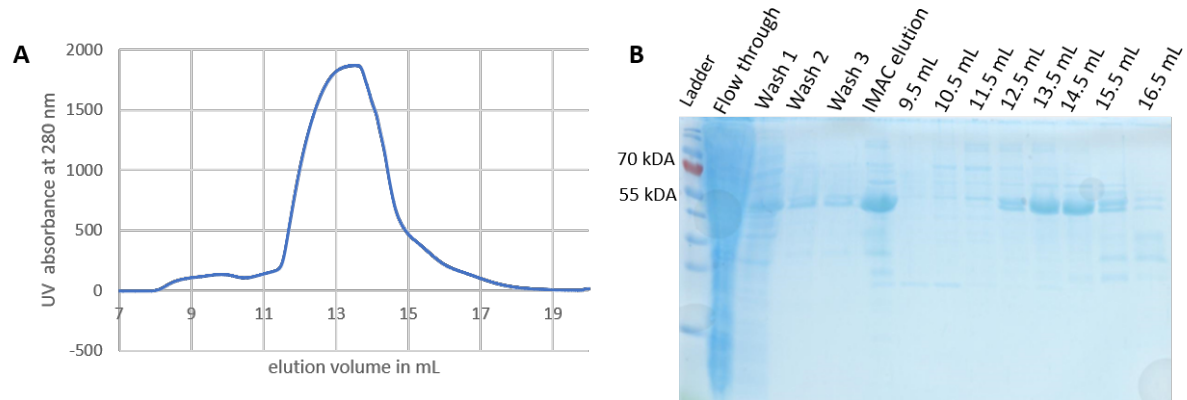


Figure 10: (A) chromatogram of SEC for FRET 148 (B) colorimetric image of 15 % SDS-PAGE with Coomassie-stained Ni-NTA purification and SEC elution fractions of FRET 148

The chromatogram of FRET 155 indicated a peak at \approx 12.5 mL (figure 11A) and fractions 12.5-15 mL were pooled.

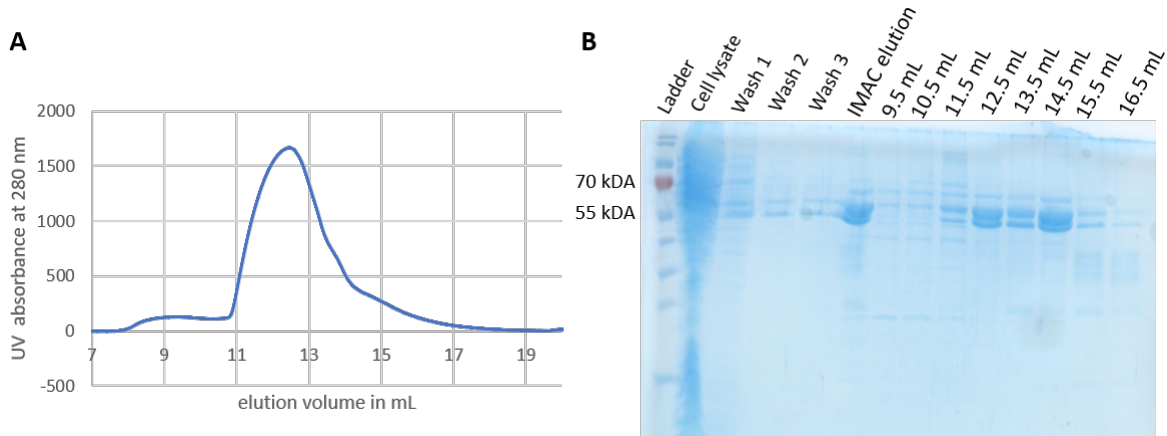


Figure 11: Chromatogram of SEC for FRET 155 (B) colorimetric image of 15 % SDS-PAGE with Coomassie-stained Ni-NTA purification and SEC elution fractions of FRET 155

Absorbance spectrum for each sensor was determined (figure 12). All sensors have an absorbance maximum at \approx 516 nm for YFP. FRET 107 and 148 displayed two peaks for CFP at appx. 435 nm and 450 nm with the CFP signal being lower than the YFP signal resulted by the extinction coefficient and quantum yield. FRET 155 was missing this signal due CFP being not folded in the expression. FRET 107 and 148 were used for further measurements and FRET 155 was expressed again.

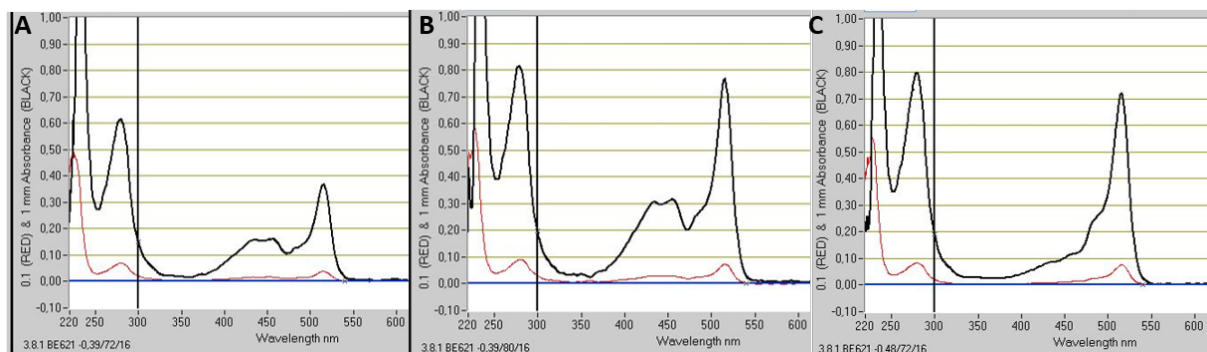


Figure 12: Absorbance spectrum for each FRET sensor of large-scale expression and purification (A)FRET 107 (B) FRET 148 (C) FRET 155

FRET 155 second Expression and Purification

FRET 155 was expressed a second time in LB- and TB-medium supplemented with 100 μ g/mL ampicillin. Samples before induction and cell harvesting were lysed by B-PER and analyzed by SDS-PAGE (figure 13). In both samples before cell harvesting a high fluorescence is visible. Therefore, the expression succeeded for both cultures.

FRET: 155 LB 155 TB

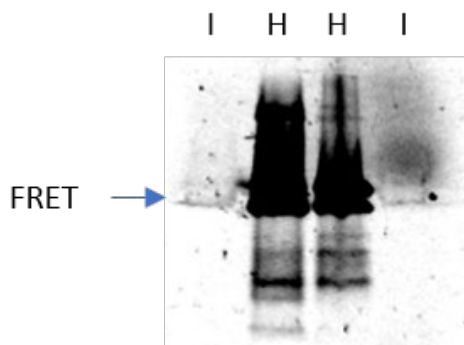


Figure 13: Fluorescence image of 15 % SDS-PAGE with lysed cells before induction and before cell harvesting for preparations for FRET 155 cultivated in LB- and TB-medium. I= sample before Induction, H= before cell harvesting

Ni-NTA purification showed a band in the elution for both samples at \approx 55 kDa (figure 14, 15). SEC displayed two peaks at appx. 9 mL and 12.5 in both cases. Due to different conformations of the sensor protein, two bands are visible. These are fainter for the expression in LB-medium. In both cases fractions from 12.5-14.5 were gathered.

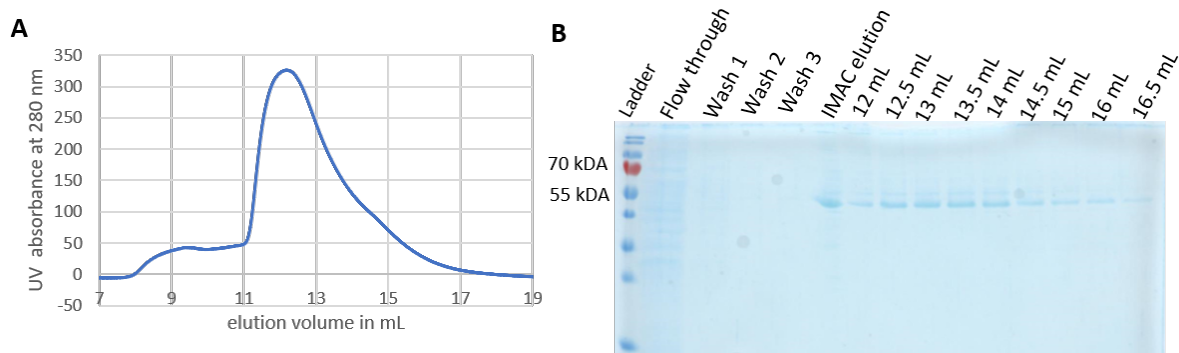


Figure 14: (A) chromatogram of SEC for FRET 155 (B) colorimetric image of 15 % SDS-PAGE with Coomassie-stained Ni-NTA purification and SEC elution fractions of FRET 155 in LB medium

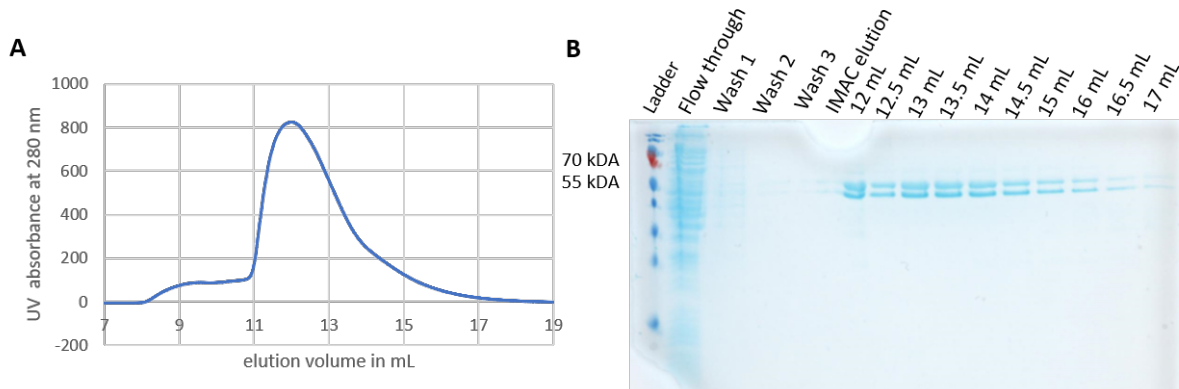


Figure 15: (A) chromatogram of SEC for FRET 155 (B) colorimetric image of 15 % SDS-PAGE with Coomassie-stained Ni-NTA purification and SEC elution fractions of FRET 155 in TB-medium

Analysis of absorbance spectra (figure 16) for both samples showed a maximum for YFP at \approx 516 nm. CFP had two maxima at appx. 435 nm and 450 nm. FRET 155 expressed in LB-Medium displayed clearer peaks for CFP and an overall higher intensity. This sample was used for further measurements.

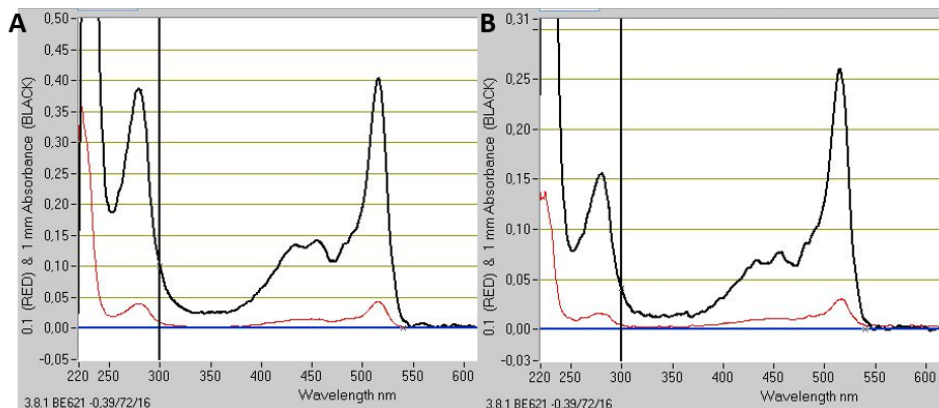


Figure 16: Absorbance spectrum for FRET 155 expressed (A) in LB-medium (B) in TB-medium

4.1.2. SecE-SpyCatcher (E-SC) expression and purification

Samples before induction with IPTG and harvesting were lysed by B-PER and analyzed via SDS-PAGE (figure 17). A successful expression is visible due to the intensive band at appx. 25-30 kDa for all samples before cell harvesting. The difference in molecular weight for each E-SC is attributed to the varying linker length of the constructs.

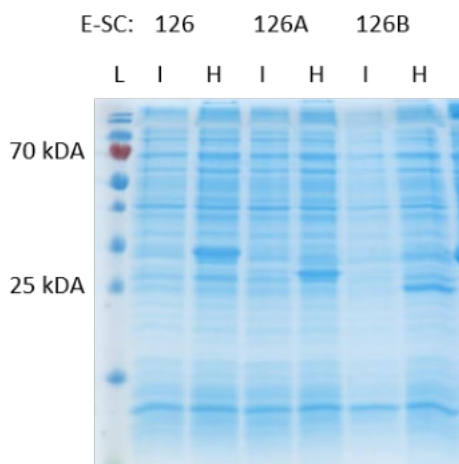


Figure 17: Colorimetric image of 15 % SDS-PAGE with Coomassie-stained lysed cells before induction and before cell harvesting for preparations for E-SC-126, 126A, 126B. L= protein ladder, I= sample before Induction, H= before cell harvesting

Harvested cells were then lysed by Microfluidizer, purified via Ni-NTA and buffer exchange (figure 18). Purified proteins after Ni-NTA are visible at appx. 25 kDa. The elution fractions for

all samples showed an intensive band for E-SC on SDS-PAGE. After buffer exchange, the band is slightly fainter due to dilution. Samples were used for further measurement. If not other mentioned, E-SC-126B construct was used.

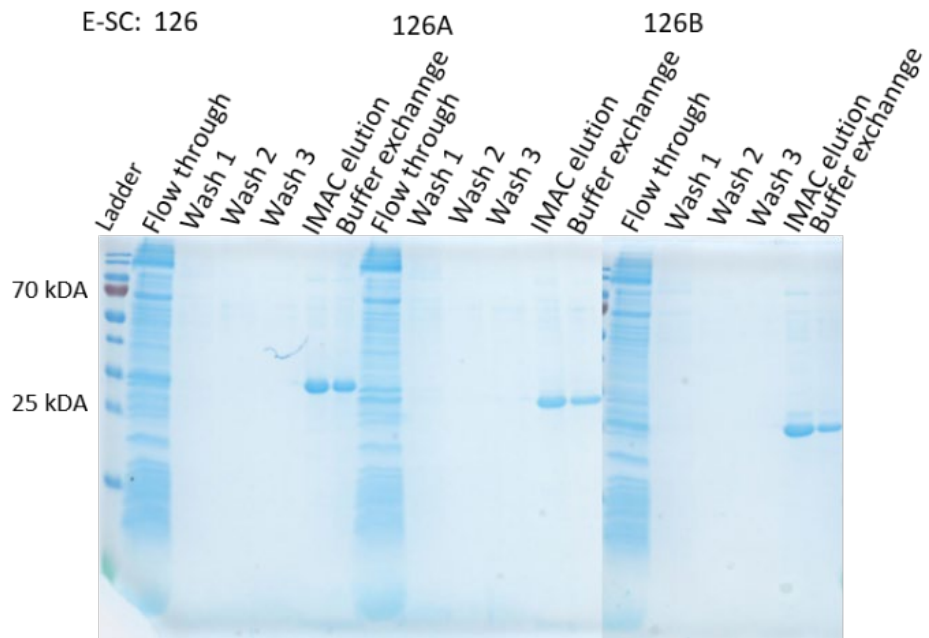


Figure 18: Colorimetric image of 15 % SDS-PAGE with Coomassie-stained Ni-NTA purification and buffer exchange for E-SC-126, 126A, 126B

4.1.3. MSP expression and purification

Cells with MSP2N2 (2N2 in the following) and MSPE3D1 (E3D1 in the following) plasmid were grown until an OD_{600} of 0.6 was reached. With B-PER lysed cells before induction and cell harvesting were analyzed via SDS-PAGE. Those samples are depicted in figure 19 together with samples from the Ni-NTA purification. 2N2 is visible at ≈ 45 kDa and E3D1 at ≈ 30 kDa. E3D1 showed a pure elution by Ni-NTA purification and was further cleaned by buffer exchange. 2N2 IMAC elution indicated impurities why it was provided by my supervisor Maryna Löwe and used for further measurements together with E3D1.

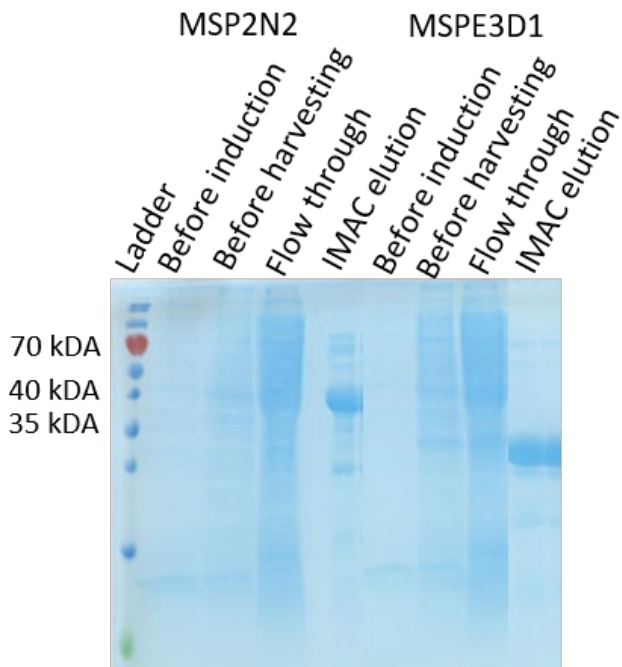


Figure 19: colorimetric image of Coomassie stained 15% SDS-PAGE with Coomassie-stained samples before induction with IPTG and cell harvesting and IMAC purification for MSP2N2, MSPE3D1

4.2. Measurements of emission spectra

By using FRET sensors in a crowded environment, macromolecular crowding could be detected. Crowding was simulated *in vitro* by using polyethylene glycol (PEG) in different sizes, Ficoll PM70 and Streptavidin (A1D3). The sensors are designed to change their conformation in a crowded environment bringing the fluorophores closer together. By exciting the donor CFP at 420 nm, the acceptor YFP was excited by the emission of CFP. With increasing crowding, CFP signal should decrease and YFP signal should increase. This leads to a higher YFP/CFP ratio.

4.2.1. FRET sensors in solution

Initial characterization of SpyTag-containing sensors was performed in solution. FRET sensors were diluted in sodium phosphate buffer with an increasing concentration of PEG4000 and Ficoll PM70 (0 %, 10 %, 20 %, 30 %, 40 %). Emission spectra were recorded via Fluorolog by exciting CFP at 420 nm.

A comparison of the FRET sensors showed that the initial signal without crowders differs from construct to construct (figure 20). CFP emission can be seen at 475 nm and YFP emission at 525 nm. FRET 107 showed the highest emission intensity for YFP and the lowest for CFP. CFP

signal for FRET 148 and 155 were the same, while FRET 155 displayed a higher YFP signal than FRET 148. Due to the flexibility in FRET 107's construct, it has a higher YFP/CFP ratio in absence of crowder. In FRET 148 and 155, the α helices lead to repulsive effect of the two arms, which decreased the energy transfer efficiency.

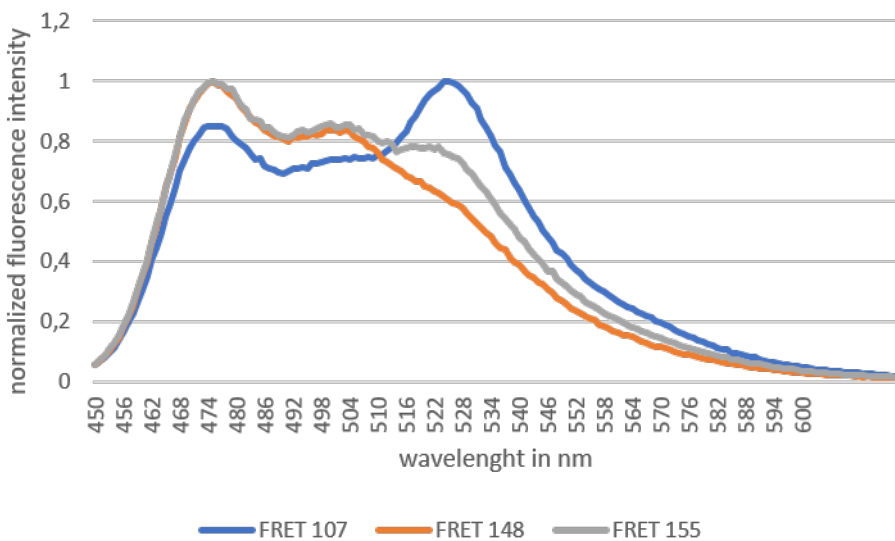


Figure 20: Emission spectra for each sensor without crowding

FRET 107 showed a gradual decrease of CFP signal with increasing crowder concentration due to successful compression of the sensor protein (figure 21).

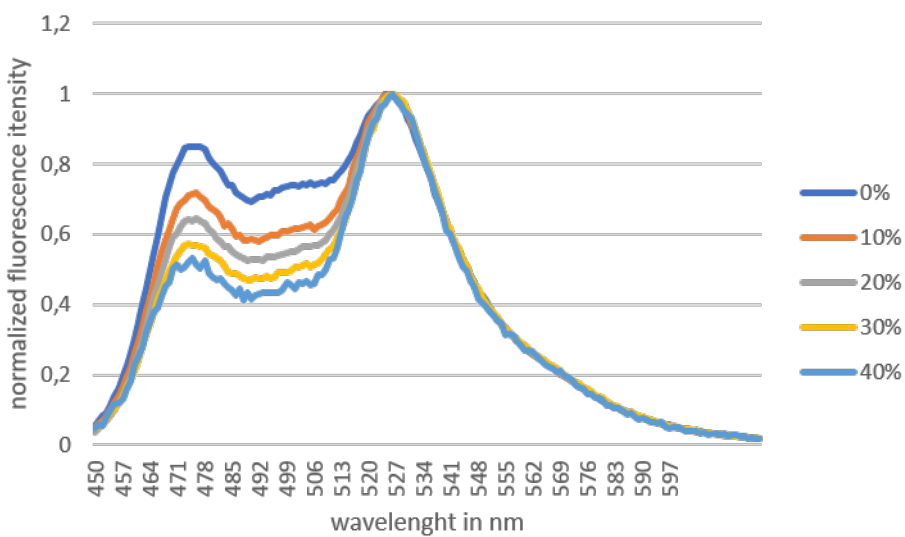


Figure 21: Emission spectra for FRET 107 in PEG4000 with different concentrations

The YFP/CFP ratios were calculated for the other sensors as well as for FRET 107 (figure 22). The ratio was calculated by the following formula with measured emissions for CFP and YFP:

$$YFP/CFP ratio = \frac{E_{525\ nm}}{E_{475\ nm} + E_{525\ nm}}$$

Higher amounts of crowding agents lead to a higher FRET ratio. For FRET 107 and 155 there is no recognizable difference between the two crowding agents. Only at 40 % the ratio was slightly higher with PEG6000. FRET 107 in 30 % Ficoll PM70 showed a sudden increase in the ratio which might be due a wrong dilution of the crowder. PEG4000 had a higher impact on FRET 148 than Ficoll PM70. At already 20 % crowder concentration, PEG4000 showed a higher ratio and got even higher.

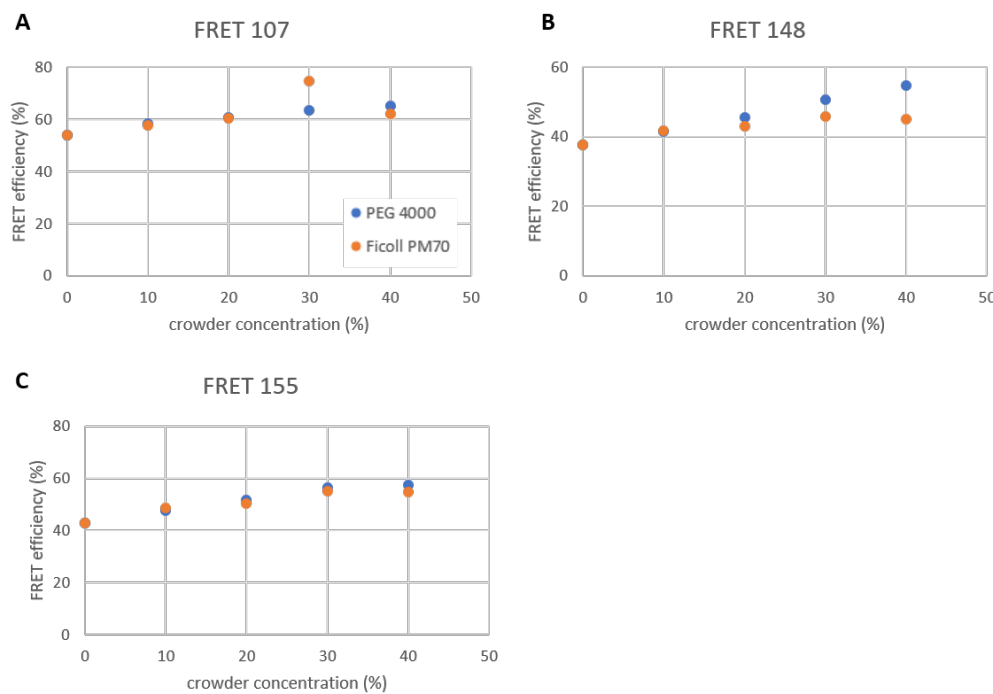


Figure 22: FRET ratio in PEG4000 and Ficoll FM70 with varying concentrations (A) for FRET 107 (B) for FRET 148 (C) for FRET 155

In addition to measuring FRET alone in solution (free FRET), FRET sensors were bound to the soluble SpyCatcher domain. For this, SpyCatcher (SpyC) was used in excess. The binding efficiency was analyzed by SDS-PAGE and the emission spectra were recorded in sodium phosphate buffer with varying concentrations of PEG4000 and Ficoll FM70 (figure 23). The SDS-PAGE (figure 23A) confirmed that all FRET sensors were able to bind completely to SpyC. This can be seen by the shift of bands to higher molecular weights. FRET sensors bound to SpyCatcher showed a band at ≈ 70 kDa, while FRET sensor in its unbound state could be found at ≈ 55 kDa.

Comparison of FRET ratios for free FRET and FRET bound to SpyC without using crowding agents (figure 23) indicated only minor variations for FRET 148 and 155. Differently, FRET 107 had a decrease of 17.2 % of YFP/CFP ratio in its SpyCatcher-bound state.

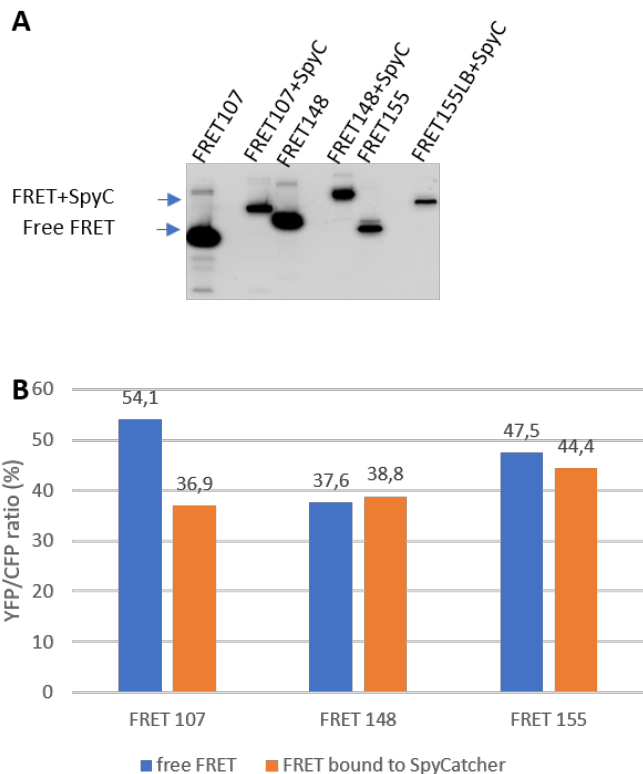


Figure 23: (A) fluorescence image of 15 % SDS-PAGE with FRET 107, 148, 155 bound to SpyC (B) comparison of FRET ratios of free FRET and FRET bound to SpyC for FRET 107, 148, 155 without crowding agents

Similarly to free sensors, an increase of crowder agents lead to higher FRET ratios in SpyCatcher-bound sensors (figure 24). Overall PEG4000 showed a higher effect on the ratio than Ficoll PM70.

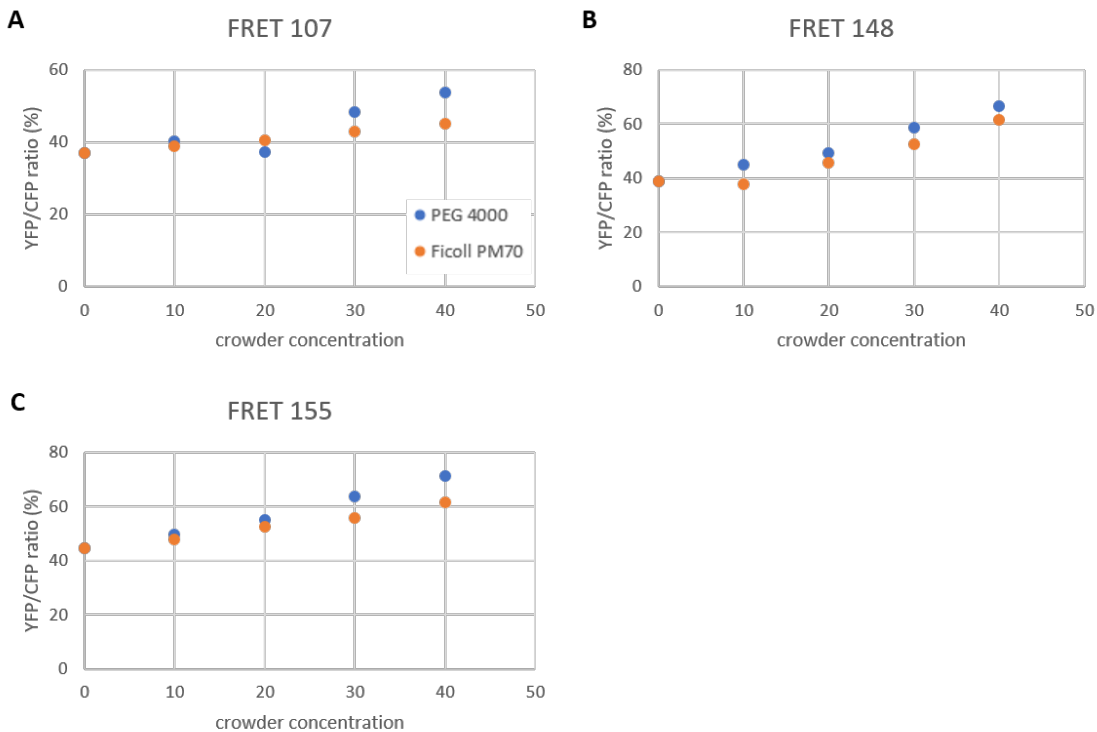


Figure 24: FRET ratio for FRET bound to SpyC in PEG4000 and Ficoll FM70 with varying concentrations A-C (A) FRET 107 (B) FRET 148 (C) FRET 155

4.2.2. FRET sensor bound to liposomes

Liposomes were prepared using DOPC (60 %) and DOPG (30 %) if not other mentioned. The remaining 10 % consisted of either DOPE, PEG5000 or DOPE-Biotin. Those proteoliposomes were designed to mimic macromolecular crowding on the cell surface. DOPE-proteoliposomes were used as a standard without crowding simulation. Liposomes with PEG covering the membrane tested the effect of the synthetic polymer as a crowder. For biotinylated liposomes, Streptavidin (A1D3) was bound to biotin on the cell surface, acting as a physiologically-relevant proteinaceous crowder. SecE-SpyCatcher-126B was reconstituted into membranes at 1:3000 mol ratio (S-EC : lipids). FRET sensors were bound to the surface by utilizing the covalent bond between SpyTag (fused with FRET sensor) and SpyCatcher (fused with transmembrane protein SecE). In this state, the emission spectra were measured and compared. However, to ensure that the FRET sensors report on the crowding at the membrane, non-bound molecules have to be removed from preparation, a task that build a large challenge within the project, as described below.

Capto Core 400 test for separation

Capto Core 400 is a multimodal chromatography which is used for purification and polishing of viruses and other large biomolecules. With this, proteoliposomes were expected to elute in the void volume, while soluble proteins bind to the column, leading to a separation of free and bound FRET sensors.

DOPE-proteoliposomes and PEG-proteoliposomes were prepared as described in methods 3.2.6. FRET 155 was bound in excess. After FRET binding, proteoliposomes were purified by multimodal chromatography with a Capto Core 400 column.

Figure 25A showed three peaks for the chromatography of DOPE-proteoliposomes at approx. 1.5, 5 and 6 mL. Those fractions were analyzed by SDS-PAGE (figure 25B). The gel displayed that, although the bound FRET sensors were enriched upon elution (2 and 4.5 mL), all fractions contained a substantial amount of free FRET 155. Hence, the trial separation of proteoliposomes from unbound FRET was not successful.

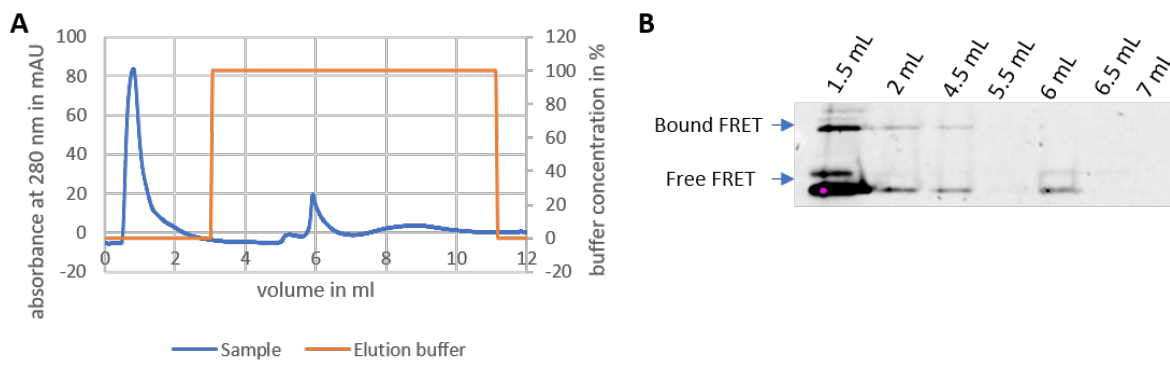


Figure 25: (A) chromatogram of multimodal chromatography for FRET 155 bound to DOPE-proteoliposomes (B) fluorescence image at 460 nm of 15 % SDS-PAGE with fractions took from the chromatography

PEG-proteoliposomes displayed similar results (figure 26). The chromatogram indicated several peaks. All elutions contained unbound FRET and again the separation failed.

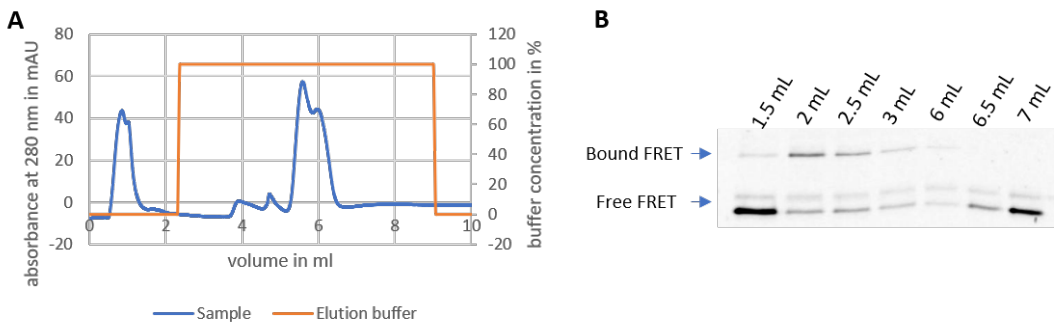


Figure 26: (A) chromatogram of multimodal chromatography for FRET 155 bound to PEG-proteoliposomes (B) fluorescence image at 460 nm of 15 % SDS-PAGE with fractions took from the chromatography

Due to failed separation of bound and unbound FRET sensors with Capto Core 400, following purifications were performed by SEC. However, optimization of the procedure, such as testing different salt concentrations in Capto Core column is possible.

Separation with SEC

SEC was used to separate unbound FRET sensors from proteoliposomes with bound FRET sensors. Proteoliposomes should elute in the void volume at approx. 8 mL due to their big size. Each FRET sensor was bound to DOPE- and PEG-proteoliposomes in excess. Samples after incubating FRET sensors with proteoliposomes (starting material) and fractions collected from SEC were analyzed by SDS-PAGE. Chosen fractions from FRET-SEC were then analyzed by Fluorolog.

Proteoliposomes with FRET 107 showed two peaks in the chromatogram at \approx 8 mL and \approx 12mL (figure 27A). PEG-proteoliposomes had a faint peak for FRET 107 bound to the E-SC at 8.5 mL, however DOPE-proteoliposomes bound with FRET 107 showed no signal (figure 27B), so likely were trapped at the filter. Unbound FRET 107 repeatedly eluted at 12.5 mL. Furthermore, emission spectra for fractions at 8.5 mL were measured (figure 27C). Both proteoliposomes showed the same signal.

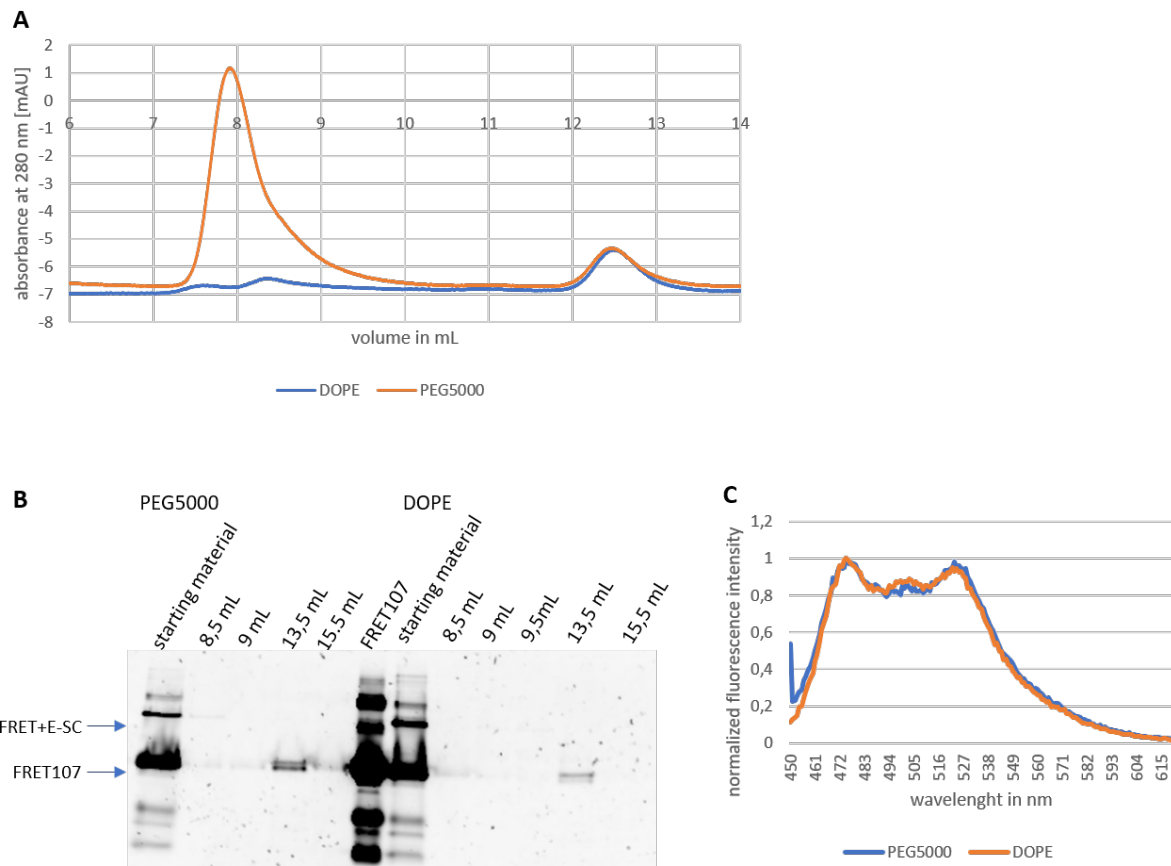


Figure 27: (A) chromatogram of SEC for DOPE- and PEG-proteoliposomes with FRET 107 (B) fluorescence image at 460 nm of 15 % SDS-PAGE with samples from SEC for FRET 107 bound to proteoliposomes (C) emission spectra of FRET 107 bound to proteoliposomes

SEC of proteoliposomes with FRET 148 indicated two peaks at appx. 8 mL and 11.5 mL (figure 28A). Both samples had bound FRET 148 in the elution at 9 mL and free FRET at 12 mL (figure 28B). Emission spectra for those elutions were measured (figure 28C). PEG had no effect to the FRET signal.

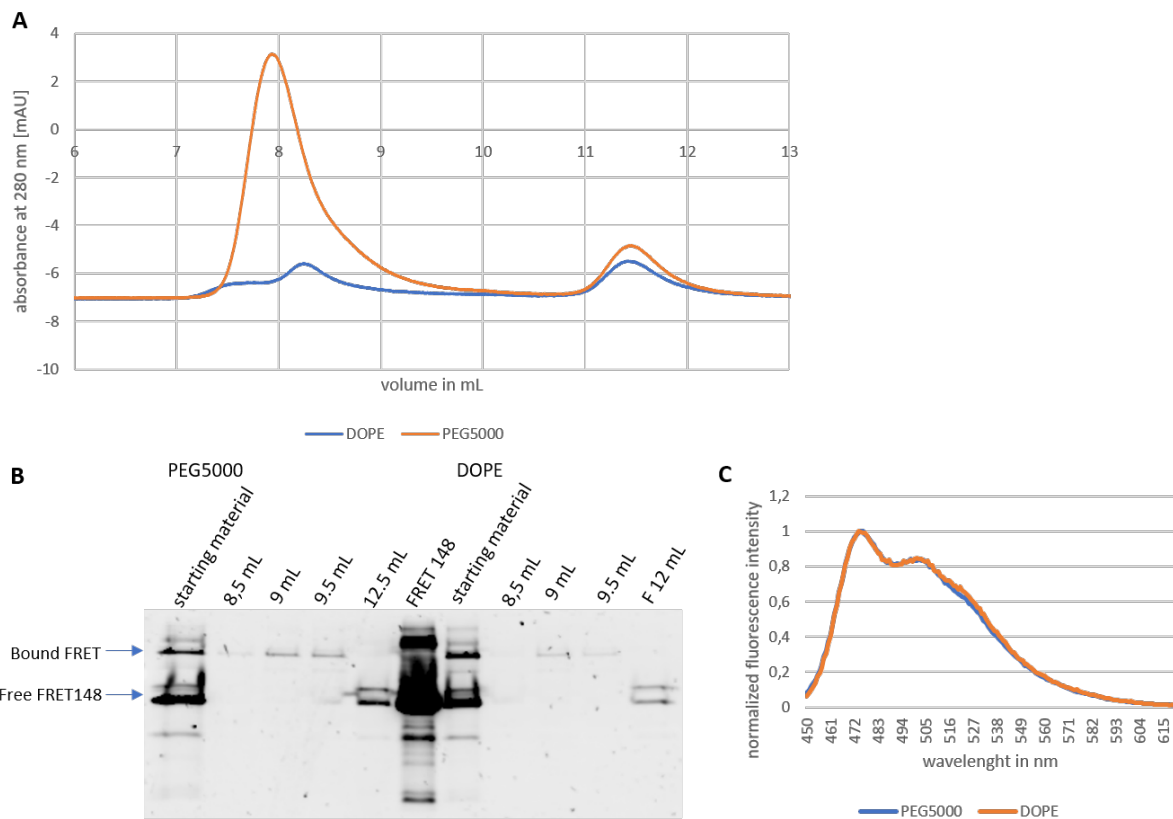


Figure 28: (A) chromatogram of SEC for DOPE- and PEG-proteoliposomes with FRET 148 (B) fluorescence image at 460 nm of 15 % SDS-PAGE with samples from SEC for FRET 148 bound to proteoliposomes (C) emission spectra of FRET 148 bound to proteoliposomes

FRET 155 indicated different peaks in both types of proteoliposomes (figure 29A). PEG-proteoliposomes had a peak at appx. 13 mL and at 19 mL, but no fluorescence signal was detected in the SDS-PAGE (figure 29B). DOPE-proteoliposomes showed peaks at appx. 9 mL, 13 mL and 19 mL, and free FRET 155 was found in elutions at 13.5 mL and 14.5 mL. FRET 155 in its bound state might be in fraction at 9 mL which was not collected. Samples at 13.5 mL were measured by Fluorolog, but the DOPE-sample contained free FRET 155 and for the PEG-sample it isn't clear if it is free or bound FRET 155.

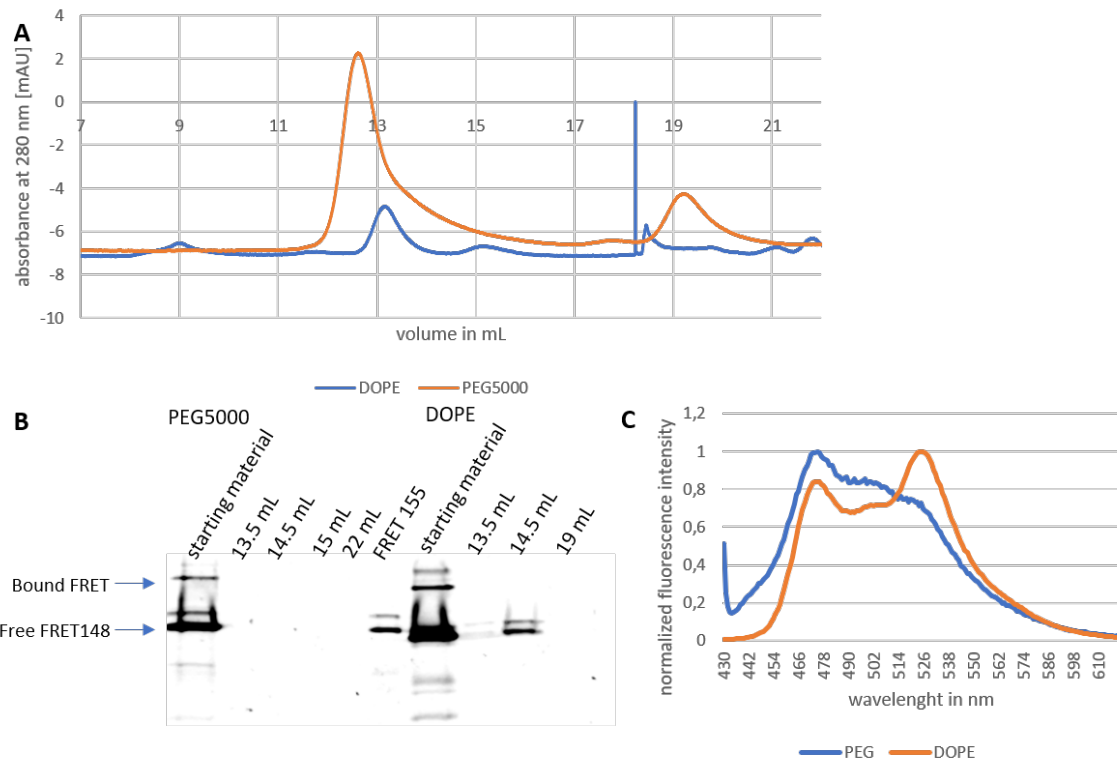


Figure 29: (A) chromatogram of SEC for DOPE- and PEG-proteoliposomes with FRET 155 (B) fluorescence image at 460 nm of 15 % SDS-PAGE with samples from SEC for FRET 155 bound to proteoliposomes (C) emission spectra of FRET 155 bound to proteoliposomes

Proteoliposomes and FRET sensor separated by SEC had indicated a loss of proteoliposomes. This might be caused by the column's filter which didn't let the particles pass through or deformed the proteoliposomes. For that reason, a modified version of separation was tested.

Separation with SEC with 100 nm proteoliposomes

To test whether smaller proteoliposomes can pass the column filter, proteoliposomes were extruded to 100 nm. After DOPE-liposome reconstitution samples were split. One sample was extruded again to 200 nm and one to 100 nm to test both sizes. FRET 155 was bound to proteoliposomes in excess. Fractions collected from SEC were analyzed by SDS-PAGE. Results are displayed in figure 30. Chromatograms for both samples had a peak at \approx 13 mL with a higher absorbance for the 100 nm sample. 200 nm sample has shown a higher absorbance at \approx 8 mL. Collected fractions were missing the signal for FRET 155 bound to proteoliposomes. Both samples had a high intensity of free FRET 155 in the 13 mL elution.

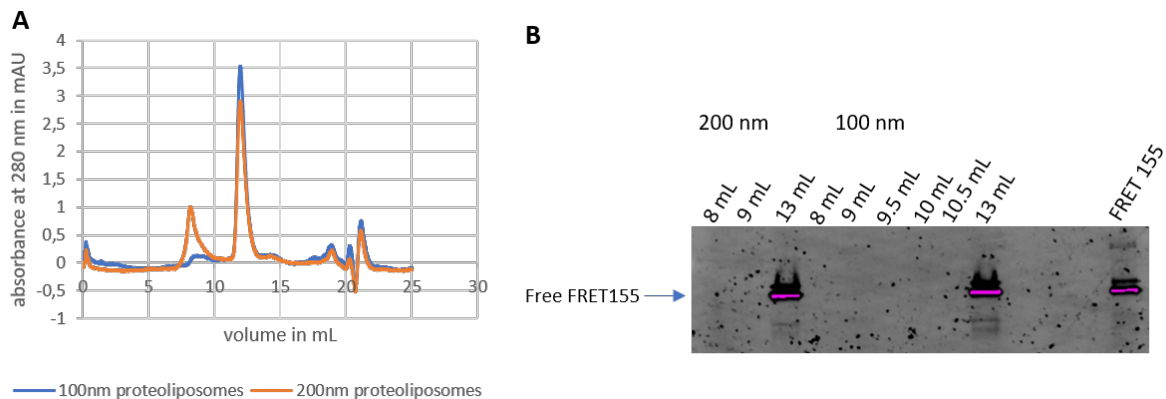


figure 30 (A) chromatogram of SEC for DOPE -proteoliposomes with FRET 155 (B) fluorescence image at 460 nm of 15 % SDS-PAGE with samples from SEC for FRET 155 bound to 100 nm and 200 nm proteoliposomes

Since this method failed as well, a new method was implemented to avoid loading of proteoliposomes on SEC column.

FRET sensor binding in low concentration

For this test DOPE- and PEG-liposomes were used. After reconstitution the proteoliposomes were sedimented at 60.000 g for 30 min. Pellets were resuspended in 100 µL sodium phosphate buffer (10 mM). We assumed that 50 % of reconstituted E-SC was facing inwards. FRET107 was added in a molar ratio of 1:5 (FRET107:E-SC) to bind E-SC molecules facing outwards. Preparations were then incubated for 4 h. A sample of 10 µL was picked for examination in 1 hour intervals. Those samples were split, for one sample the binding was stopped by adding SDS-PAGE sample buffer and for the other one the emission spectrum was measured. In addition, the preparations were incubated for 24 h.

Figure 31A,B showed the binding process of FRET 107 to proteoliposomes containing DOPE and PEG. The intensity of the bands of free and E-SC bound sensor were measured and plotted against the time (figure 31C,D). A gradual decrease of free FRET 107 is visible in DOPE-preparation. Accordingly FRET 107 in its bound state increases. PEG-preparation displayed irregular values for the band intensity. This may also be caused due to the high crowding on the cell surface by PEG because it leads to a higher repulsion on the cell surface wherefore FRET 107 cannot reach SpyCatcher.

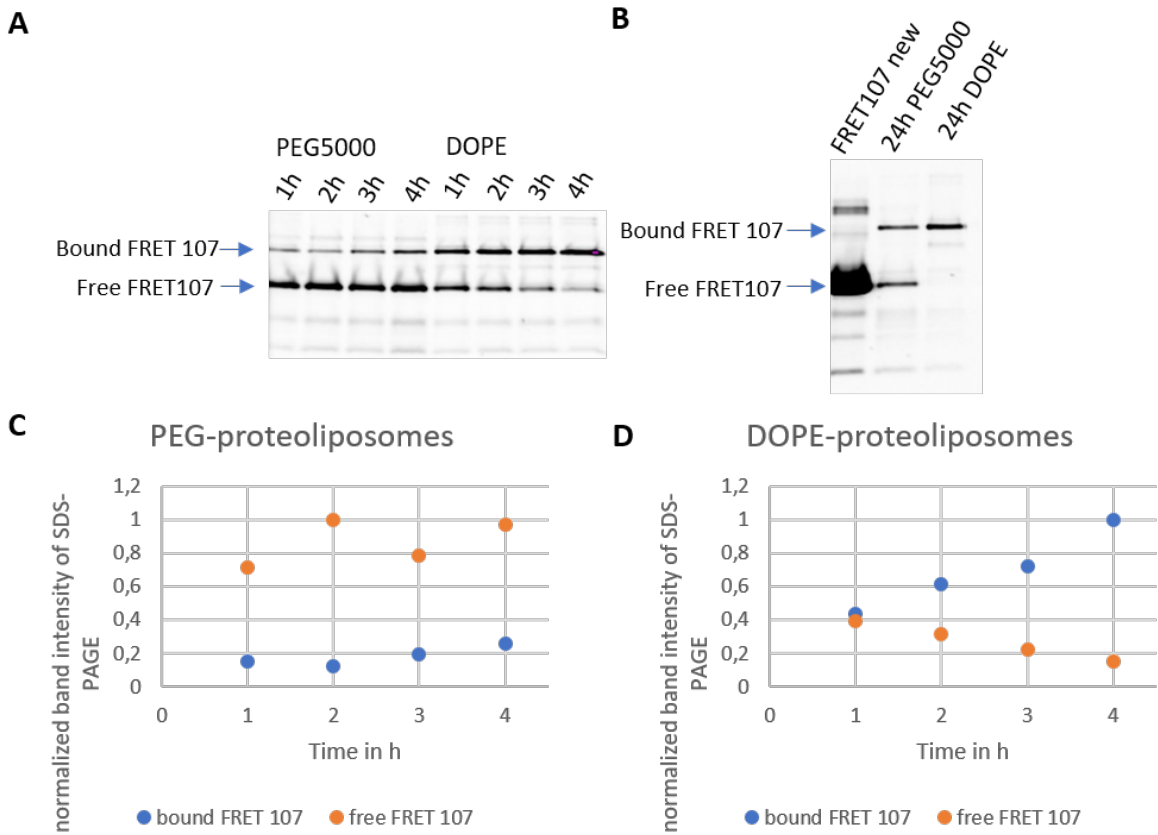


Figure 31: (A) fluorescence image at 460 nm of 15 % SDS-PAGE with samples picked each hour for PEG- and DOPE-proteoliposomes with FRET 107 (B) fluorescence image at 460 nm of 15 % SDS-PAGE with samples picked after 24 h for PEG- and DOPE-proteoliposomes with FRET 107 (C) band intensities for samples took each hour for PEG-proteoliposomes (D) band intensities for samples took each hour for DOPE-proteoliposomes

The emission spectra for each preparation showed two peaks (figure 32). Donor CFP emitted at appx. 472 nm and acceptor YFP at appx. 525 nm. We expected a decrease of CFP signal in crowded environment. Due to more bound sensors than free sensors after each hour, the energy transfer of CFP to YFP should have led to an increase in YFP signal and decrease of CFP signal. In our measurement, this was not observed but instead after each hour, the CFP signal increased and with that the YFP/CFP ratios decreased for both preparations.

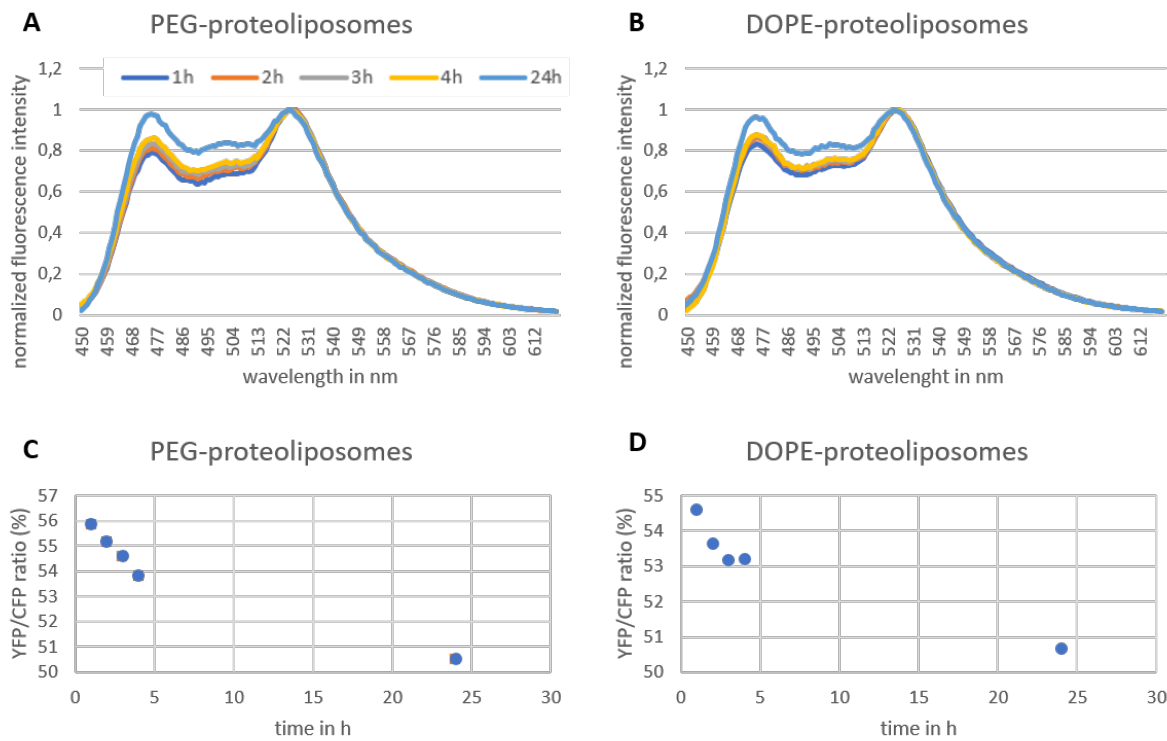


Figure 32: Emission spectra and YFP/CFP ratios for FRET 107 (A)(C) preparation with PEG-proteoliposomes (B)(D) preparation with DOPE-proteoliposomes

This test was repeated three times with DOPE- and Biotin-proteoliposomes. Each FRET sensor was bound as described before. Samples after 4 h were checked by 15 % SDS-PAGE (figure 33). For each repetition intensive bands of free FRET sensors were still visible. The binding was not as successful as before due to unknown reasons.

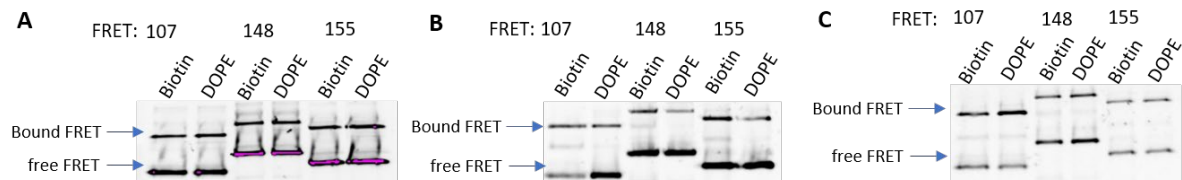


Figure 33: Fluorescent image at 460 nm of 15 % SDS-PAGE with FRET 107, 148, 155 to DOPE- and biotin-proteoliposomes after 4 h incubation (A) first try (B) second try (C) third try

Hence the results were not reproducible, an alternative procedure of preparing proteoliposomes was tried.

Complex formation of FRET and E-SC before reconstitution

Each FRET sensor was added to E-SC in excess. After 4 h incubation, the samples were injected to SEC column to separate FRET sensor-E-SC complex from unbound proteins. Those samples were analyzed by SDS-PAGE (figure 34).

FRET 107-E-SC complex showed three peaks at appx. 10, 14 and 16 mL (figure 34A). Elution fractions with only bound FRET sensor could be found at 10.5-13.5 mL. Elutions 10.5-13 mL has displayed bright bands and were pooled for further measurements. (figure 34D)

FRET 148-E-SC complex had several overlapping peaks at \approx 10 mL and a second one at \approx 13 mL (figure 34B). Elutions at 9-11.5 mL has displayed intensive bands with bound FRET sensor and were pooled together for further measurements (figure 34E).

FRET 155-E-SC complex indicated similar peaks as FRET 148-E-SC complex (figure 34C). Elution at 9.5-12.5 mL had intensive bands for bound FRET sensor and were pooled for further measurements (figure 34E). However, elution at 10 mL has shown a double band and was discarded.

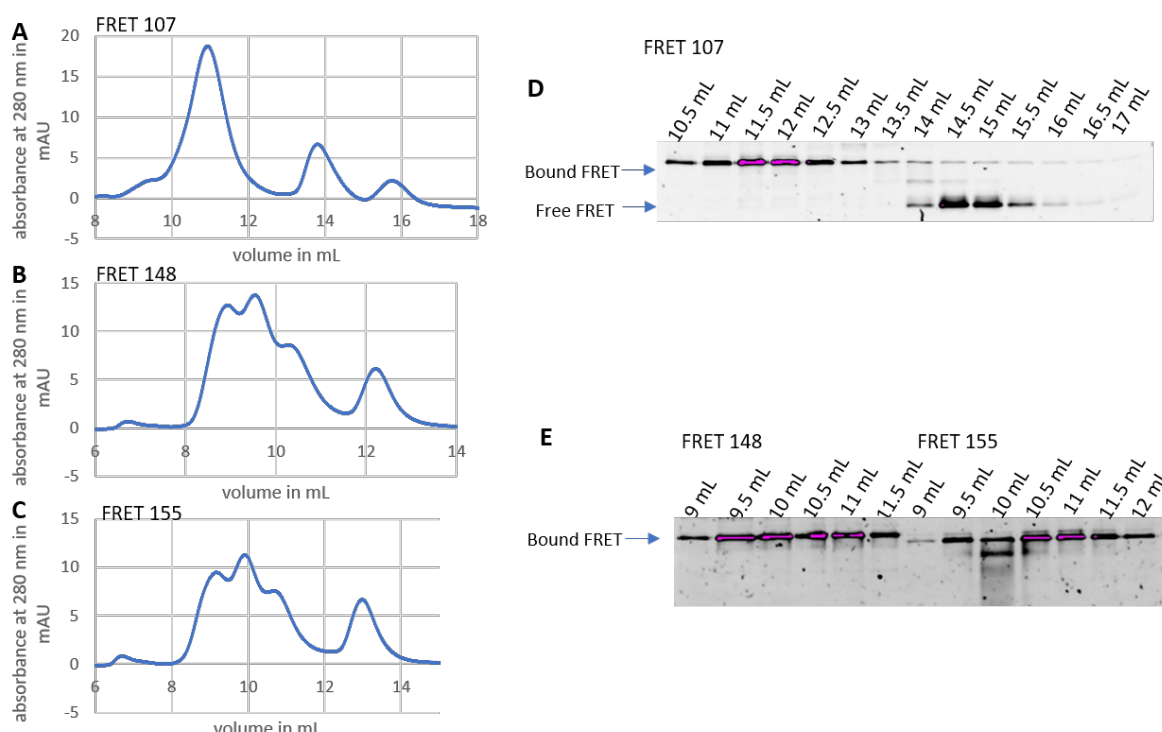


Figure 34: Chromatogram of SEC for FRET sensor bound to E-SC (A) FRET 107 (B) FRET 148 (C) FRET 155; Fluorescence image at 460 nm of elution fractions from SEC for FRET sensor bound to E-SC (D) FRET 107 (E) FRET 148, 155

Samples with the bound complex were then reconstituted into DOPE-, PEG- and Biotin liposomes. After reconstitution, proteoliposomes were centrifuged (AT3 rotor) at 60.000xg for 30 min. The pellet was resuspended in 100 µL lipid buffer and emission spectra were measured by Fluorolog. Furthermore, A1D3 was added to Biotin samples as described in methods 3.2.8. Samples before centrifugation (starting material) and after centrifugation (from supernatant and resuspended pellet) were analyzed by SDS-PAGE (figure 35). Proteoliposomes could be found in resuspended pellets, and FRET sensor complexes which did not bind in the supernatant. After pelleting proteoliposomes, every sample showed several bands. FRET 107 and FRET 148 bound to PEG-proteoliposomes already displayed extra bands in the starting material which decreased in the pellet. Biotinylated proteoliposomes indicated several bands in the pellet.

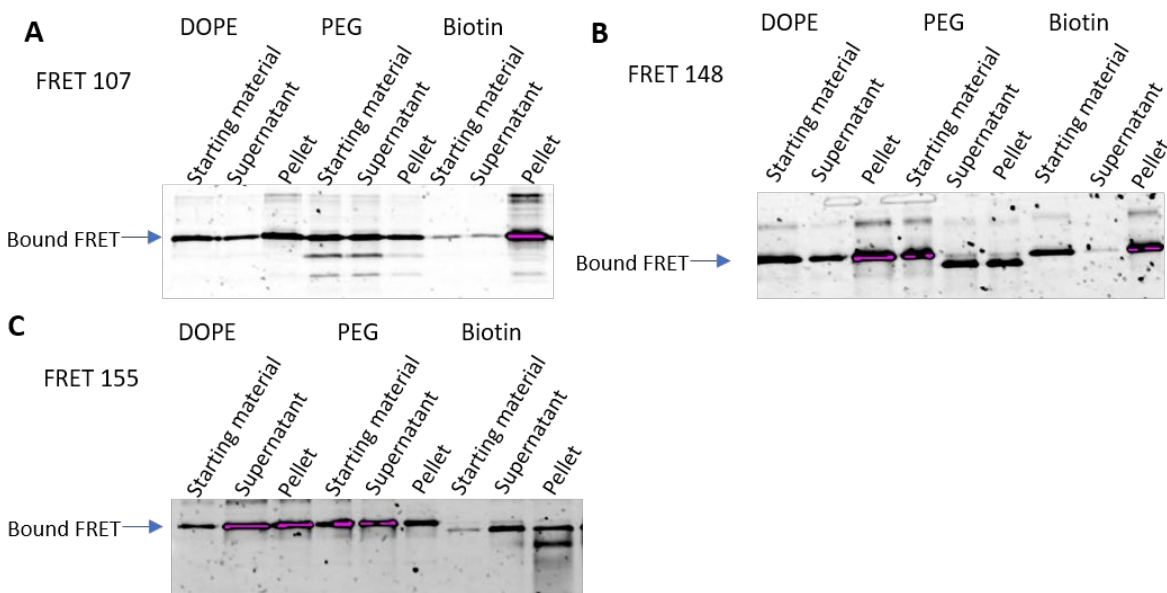


Figure 35: fluorescence image at 460 nm for 15 % SDS-PAGE with starting material, supernatant and resuspended pellet of DOPE-, PEG-, Biotin-proteoliposomes bound with FRET sensor (A) FRET 107 (B) FRET 148 (C) FRET 155

Resuspended pellets were then measured by Fluorolog. Biotin-proteoliposomes were measured with A1D3 and without. All samples had two pronounced peaks at 475 nm (CFP) and 525 nm (YFP) (figure 36,37,38).

FRET 107 showed a distinct difference between fluorescence intensities of CFP and YFP (figure 36). PEG-proteoliposomes had the highest YFP/CFP ratio signal resulted by the more compressed form of the sensor in comparison to DOPE proteoliposomes. FRET ratio for DOPE-proteoliposomes was slightly higher than for Biotin-proteoliposomes and adding the crowding agent A1D3 further decreased the ratio; however the variations were rather small.

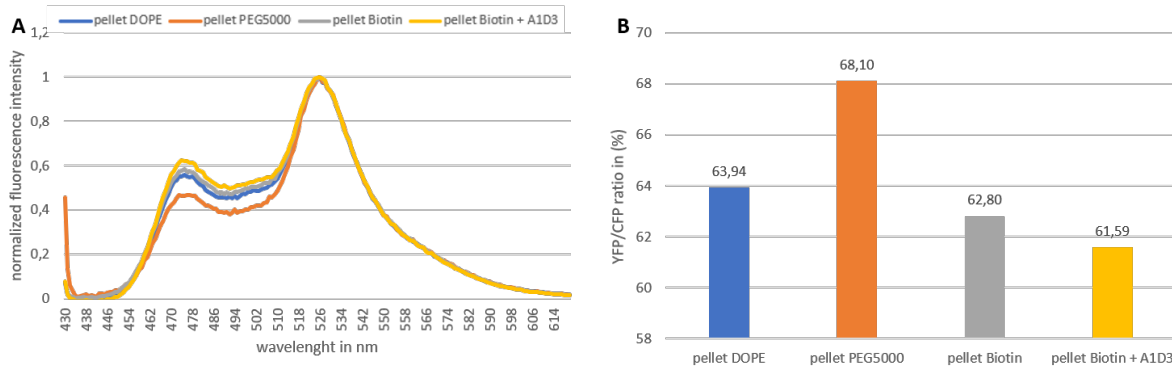


Figure 36: (A) emissions spectra and (B) CFP/YFP ratio for FRET 107 bound to DOPE-, PEG and Biotin-proteoliposomes

Similarly, FRET 148 bound to PEG-proteoliposomes has shown a substantial increase in YFP fluorescence (figure 37). Remaining proteoliposomes had similar spectra with a higher CFP signal indicating a low energy transfer with minor variations in FRET efficiency.

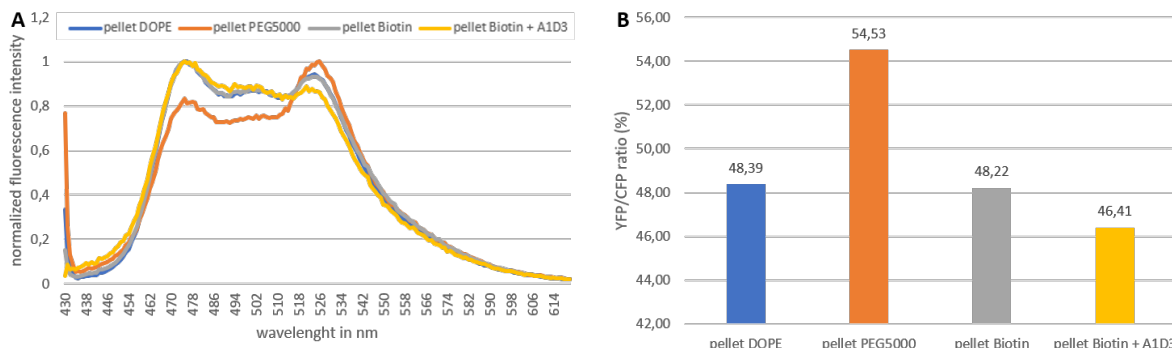


Figure 37: (A) emissions spectra and (B) CFP/YFP ratio for FRET 148 bound to DOPE-, PEG and Biotin-proteoliposomes

FRET 155 had the lowest FRET ratio for PEG-proteoliposomes (figure 38). Remaining proteoliposomes gave almost same signals for YFP and CFP with YFP signal being higher.

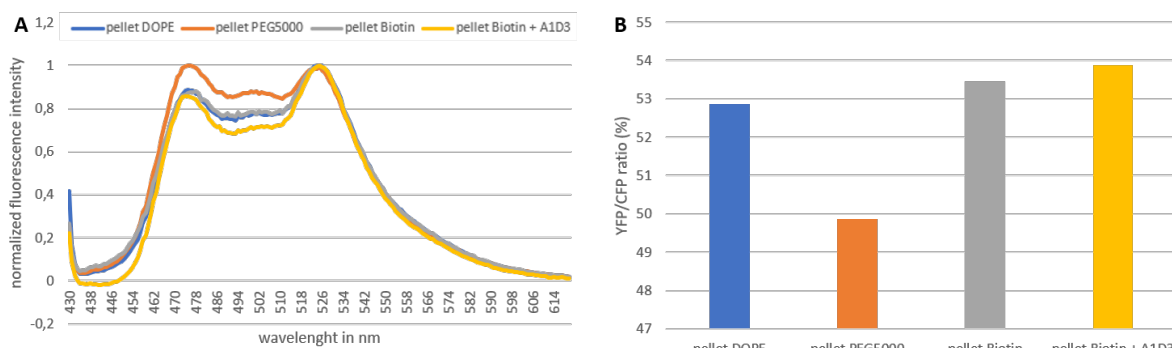


Figure 38: (A) emissions spectra and (B) CFP/YFP ratio for FRET 155 bound to DOPE-, PEG and Biotin-proteoliposomes

Binding FRET sensor to E-SC before reconstitution displayed unexpected results. As expected, PEG has shown a substantial increase in FRET efficiencies for sensors 107 and 148, but with FRET 155 it led to an increase of the signal. Furthermore, the crowder A1D3 barely affected the FRET efficiency for all examined sensors.

In addition to proteoliposomes, Nanodiscs were used in the following measurements.

4.2.3. FRET sensors bound to Nanodiscs

Nanodiscs were prepared as described in methods 3.2.6. A test SEC was carried out with E3D1 Nanodiscs to determine at which volume Nanodiscs can be eluted. Nanodiscs were prepared in a molar ratio of 1:25 and 1:50 (E3D1:lipids) and injected to SEC column (figure 39). Both samples eluted at appx. 11 mL. Nanodiscs with a 1:50 ratio eluted first, likely due to larger surface area.

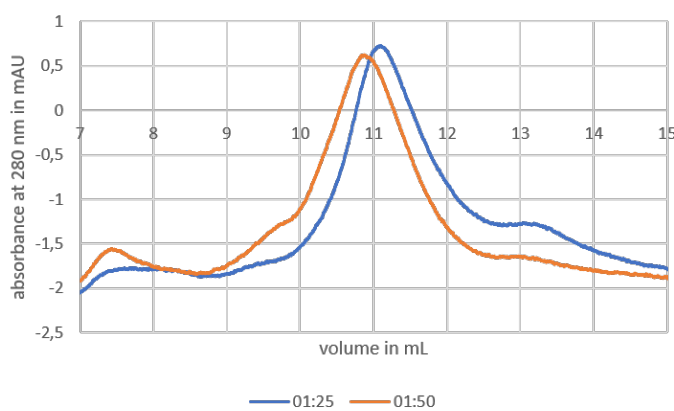


Figure 39: Chromatograms of SEC for E3D1 DOPE-Nanodiscs in different sizes

Separation with SEC

E3D1 and 2N2 Nanodiscs with DOPE-, PEG- and Biotin-containing lipids were reconstituted as described in methods 3.2.6. FRET 107 was bound to E3D1 Nanodiscs, and FRET 148, 155 to 2N2 Nanodiscs. Preparations were centrifuged at 14.860xg for 15 min to sediment occasional proteoliposomes, and the supernatant was loaded on SEC. Before, A1D3 was added to biotinylated Nanodiscs and incubated for 30 min. Elution fractions were analyzed by SDS-PAGE.

FRET 107 bound to Nanodiscs eluted at 10 mL (DOPE- and Biotin-Nanodiscs) and 9.5 mL (PEG-Nanodiscs) (figure 40). PEG Nanodiscs eluted earlier probably due to an increase of size caused by PEG5000. For each preparation at 14.5 mL free FRET 107 could be detected. Emission spectra for samples with bound FRET 107 were measured. PEG-Nanodiscs has shown the highest YFP/CFP ratio. Similar spectrum was measured for DOPE-Nanodiscs. Biotinylated Nanodiscs displayed a slightly higher CFP signal than free FRET with the lowest ratio.

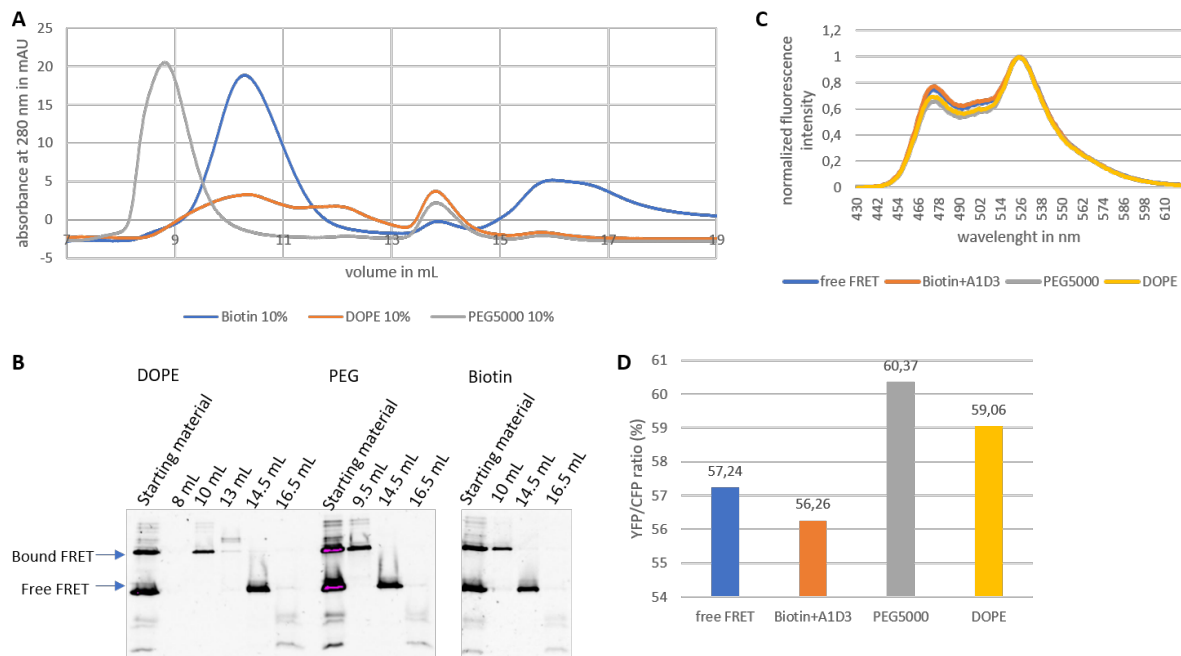


Figure 40: (A) chromatogram for DOPE-, PEG- and Biotin-Nanodiscs with FRET 107 (B) fluorescence image at 460 nm of 15 % SDS-PAGE with sample after centrifugation and elution fractions after SEC for FRET 107 (C) emission spectra for FRET 107 and FRET 107 bound to DOPE-, PEG- and Biotin-Nanodiscs (D) YFP/CFP ratios for FRET 107 bound to proteoliposomes

FRET 148 in its bound state eluted at 10 mL (DOPE-Nanodiscs), 9.5 mL (PEG-Nanodiscs) and 10.5 mL (Biotin-Nanodiscs) (figure 41). Elution of free FRET sensor was again at 14.5 mL. Emission spectra for samples with bound FRET 148 were measured. All samples showed the same spectra with slight difference to free FRET 148.

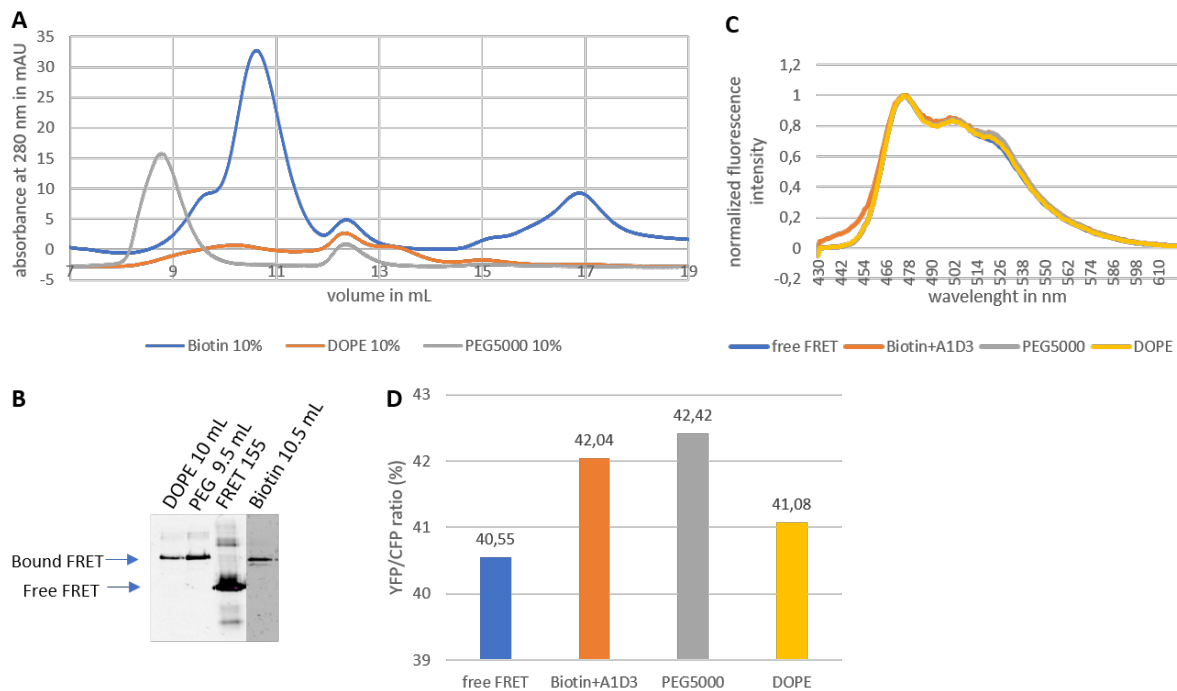


Figure 41: (A) chromatogram for DOPE-, PEG- and Biotin-Nanodiscs with FRET 148 (B) fluorescence image at 460 nm of 15 % SDS-PAGE with sample after centrifugation and elution fractions after SEC for FRET 148 (C) emission spectra for FRET 148 and FRET 148 bound to DOPE-, PEG- and Biotin-Nanodiscs (D) YFP/CFP ratios for FRET 148 bound to different proteoliposomes

Chromatogram for FRET 155 indicated the same elution pattern as FRET 148. In its bound state it eluted at 10 mL (DOPE-Nanodiscs), 9.5 mL (PEG-Nanodiscs) and 10.5 mL (Biotin-Nanodiscs) (figure 42). Elution of free FRET 155 was again at 14.5 mL. Emission spectra for samples with bound FRET 155 were measured. PEG- and DOPE-Nanodiscs showed the same CFP:YFP signal with the highest ratio. Biotinylated Nanodiscs with A1D3 led to a decrease in YFP signal and indicated a lower ratio than free FRET.

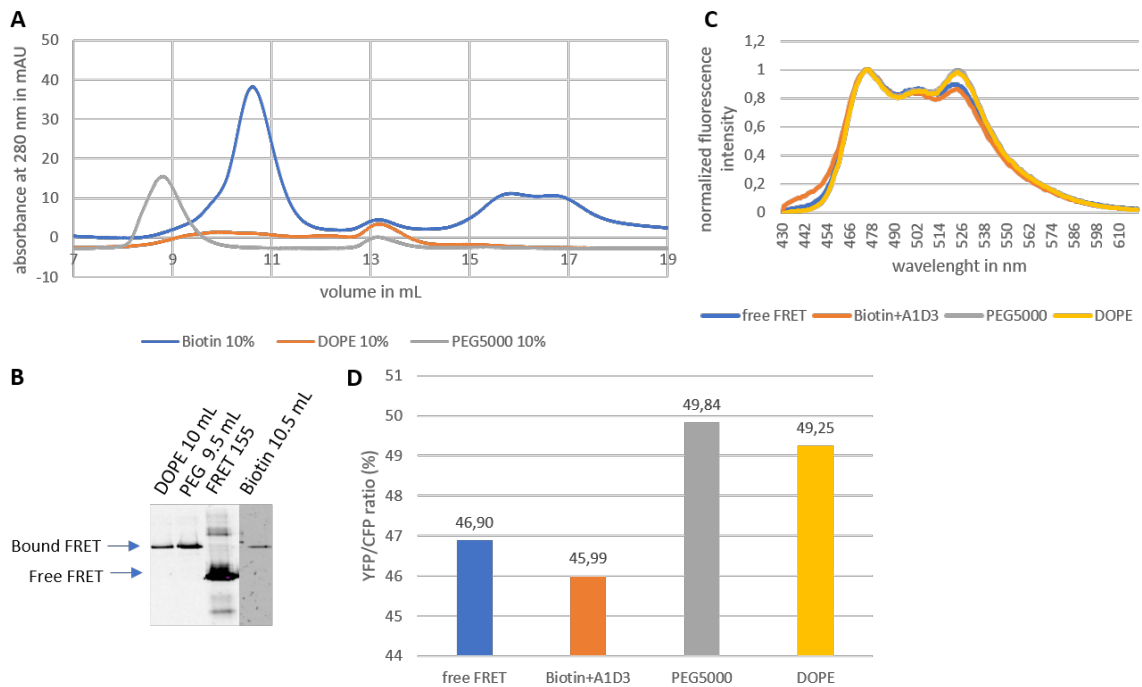


Figure 42: (A) chromatogram for DOPE-, PEG- and Biotin-Nanodiscs with FRET 155 (B) fluorescence image at 460 nm of 15 % SDS-PAGE with sample after centrifugation and elution fractions after SEC for FRET 155 (C) emission spectra for FRET 155 and FRET 155 bound to DOPE-, PEG- and Biotin-Nanodiscs (D) YFP/CFP ratios for FRET 155 bound to different proteoliposomes

Testing FRET sensors on Nanodiscs has not provided expected results. Due to the low FRET signal with the crowder A1D3, its binding to biotinylated Nanodiscs was tested.

A1D3 bound to Nanodiscs

E3D1 Nanodiscs with 1 %, 5% and 10 % Biotin were prepared to test the binding efficiency of A1D3. For this E-SC-126A was reconstituted into the Nanodiscs and FRET 107 was added in excess. After FRET sensor binding, A1D3 was added in a molar ratio of 1:2 (A1D3:10 % Biotin) for all preparations and incubated for 30 min. Samples with A1D3 bound to Nanodiscs were then purified by SEC and elutions were analyzed by SDS-PAGE (figure 43). SEC showed three peaks at appx. 11 mL, 14 mL and 17 mL. Nanodiscs with bound FRET 107 eluted at \approx 11 mL, free FRET 107 at 15 mL and unbound A1D3 at 17 mL. With an increase of biotin in Nanodiscs, the amount of unbound A1D3 decreased. When comparing the peaks at 11 mL and 17 mL, a loss of A1D3 is visible. Coomassie stained image displayed FRET bound to E-SC at \approx 70 kDa, A1D3 at \approx 66 kDa and MSPE3D1 at \approx 26 kDa (figure 43C).

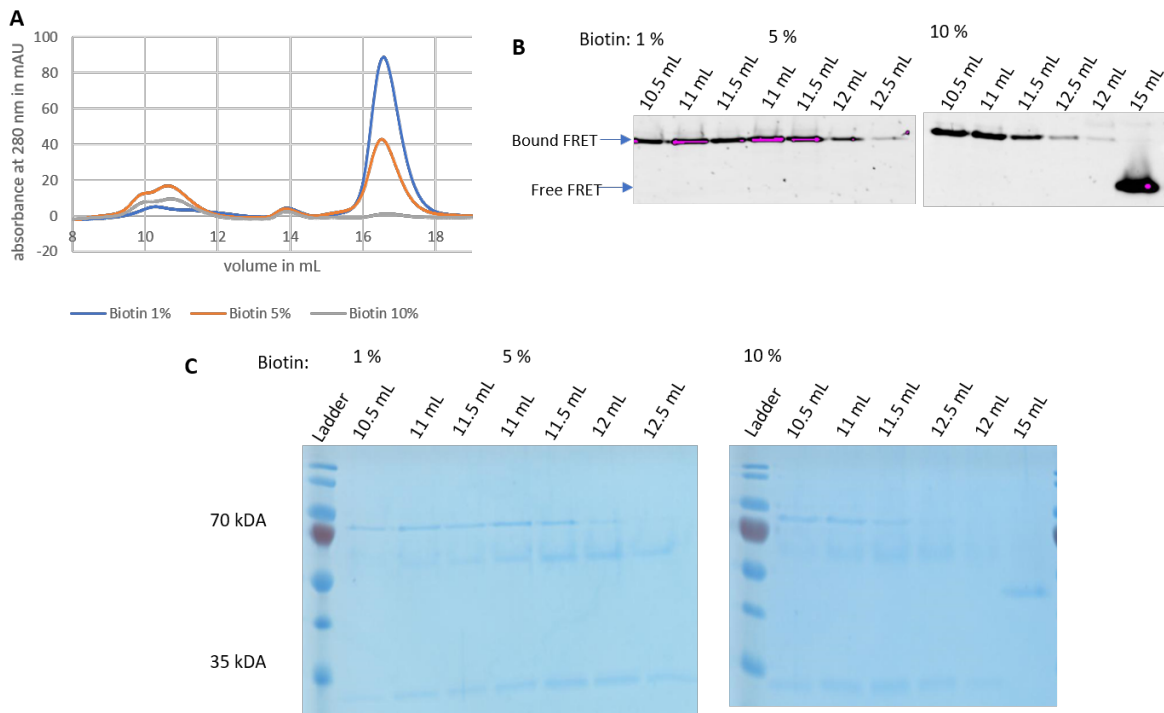


Figure 43: (A) chromatograms of SEC for FRET 107 and A1D3 bound to Nanodiscs with different amounts of Biotin; 15 % SDS-PAGE with elution fractions from SEC (B) fluorescence image at 460 nm (B) colorimetric image with Coomassie-stained unboiled samples of FRET 107 and A1D3 bound to Nanodiscs

Emission spectra for elutions at 11 mL were then recorded (figure 44). All preparations showed the same FRET signal, thus the presence of the surface-bound A1D3 had no effect on nanodisc-incorporated FRET 107.

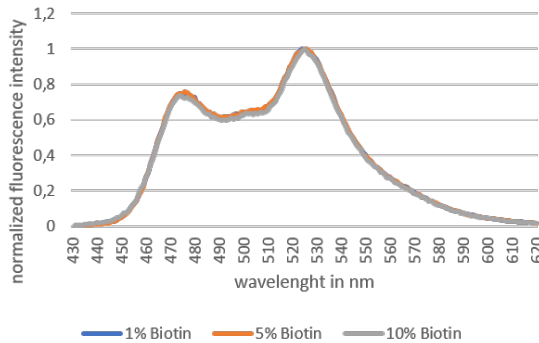


Figure 44: Emission spectra for FRET 107 bound to Nanodiscs with different amounts of Biotin

4.3. Additional measurements of emission spectra

One likely explanation of the poor performance of the membrane-bound FRET sensors is their separation from the membrane interface determined by the SpyCatcher domain (diameter approx. 2 nm), but also the membrane linker. SecE in its native environment with SecYG is stabilized by the translocon. Without, a part of SecE reaches out of the synthetic

membrane and leads to higher gap between FRET sensor and membrane. For this reason, proteoliposomes with thicker bilayers were manufactured to provide a complete integration of SecE, minimizing the gap.

Liposomes with 22:1 PC (80 %), DOPG (10%) and either DOPE-PEG5000 (10%) or DOPE (10%) were manufactured. FRET sensor-E-SC complexes with FRET 148 and 155 were reconstituted in those liposomes and centrifuged (AT3) at 60.000xg for 30 min. Pellets were resuspended in 100 µL Lipid buffer and analyzed by SDS-PAGE to confirm that FRET was bound to proteoliposomes (figure 45A). Emission spectra were measured by Fluorolog. The emission spectra (figure 45B,C) for both preparations did not show a difference between PEG- and DOPE-proteoliposomes.

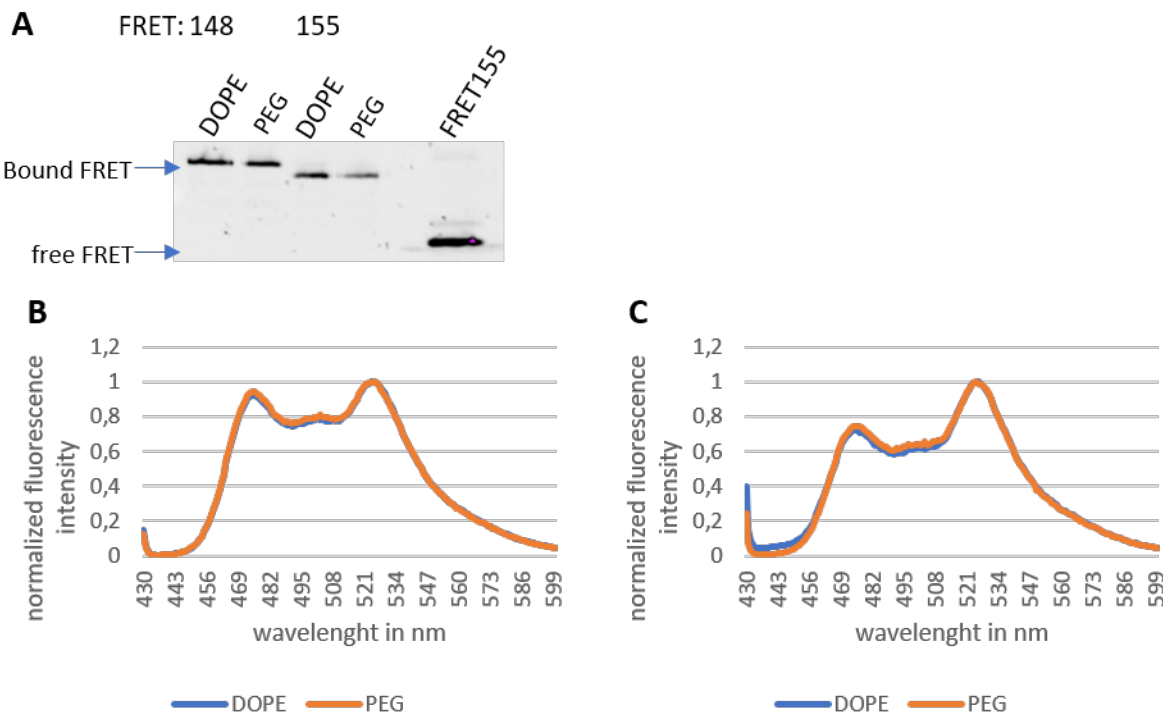


Figure 45: (A) fluorescence image at 460 nm of SDS-PAGE with FRET 148 and 155 bound to DOPE- and PEG-proteoliposomes; Emission spectra for FRET sensors bound to DOPE- and PEG proteoliposomes (B) FRET 148 (C) FRET 155;

4.4. EmrE-SpyCatcher, EmrE-YFP expression and purification

EmrE-SpyCatcher expression and purification

In a search for a shorter membrane anchor, transmembrane domains 1 and 2 of *E. coli* EmrE was chosen as a substitute for SecE. Cells with a plasmid encoding for EmrE-SpyCatcher were

grown until an OD₆₀₀ of 0.6 was reached. Ni-NTA trial purification with samples was performed. Three preparation were washed with Wash buffer Catcher containing 10 mM, 20 mM, 30 mM imidazole and analyzed by SDS-PAGE (figure 47). All preparations have shown a range of bands in the elution. Elution bands became fainter with increasing imidazole concentration due to more loss of protein in the washing step. Furthermore, samples took from the elution were mixed with FRET 107 to examine SpyTag/SpyCatcher binding. When comparing the band of free FRET 107 to EmrE-SpyCatcher mixed with FRET 107, there was no shift towards higher molecular mass observed which indicated the failed binding. With the assumption that EmrE-SpyCatcher was not expressed, a new expression with EmrE-YFP was prepared to check the expression of EmrE.

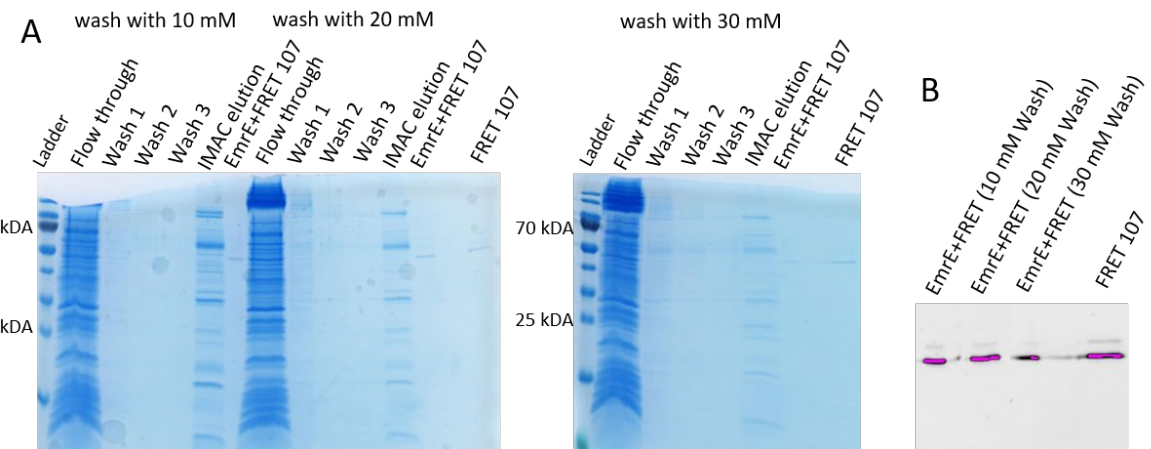


Figure 46: (A) colorimetric image of 15 % SDS-PAGE with Coomassie-stained samples from Ni-NTA purification washed with 10 mM, 20 mM, 30 mM imidazole (B) fluorescence image at 460 nm of EmrE-SpyCatcher+FRET 107 binding

EmrE-YFP

Two preparations of cells with a plasmid encoding EmrE-YFP were grown and expressed at 30 °C and 37 °C. Harvested cells of both preparations were lysed each by B-PER and glass beads. Samples were analyzed by SDS-PAGE. Only cells lysed by B-PER have shown a faint signal for EmrE-YFP. Cells grown at 30 °C have displayed a band while cells at 37 °C have shown a fluorescence signal of unknown nature (figure 47).

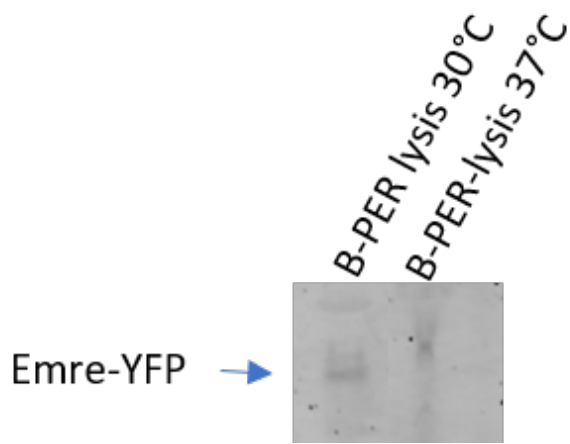


Figure 47: Fluorescence image at 460 nm of 15 % gel with EmrE-YFP cells lysed by B-PER

EmrE-SpyCatcher and -YFP second expression

In the second expression of EmrE-SpyCatcher and -YFP, isolated membranes were analyzed by SDS-PAGE (figure 48). Surprisingly, both samples have shown fluorescence at 70 kDa. Fainter bands can be seen further down. EmrE-SpyCatcher should not result in a fluorescence signal, while EmrE-YFP fusion protein should be at appx. 25 kDa. Potentially, the fluorescence signal observed in the first trial expression (figure 47) corresponded to EmrE-YFP in cytoplasm, so the membrane targeting and integration was not accomplished. Further screening of the expression conditions or alternative membrane anchors may be required to achieve an optimized construct.

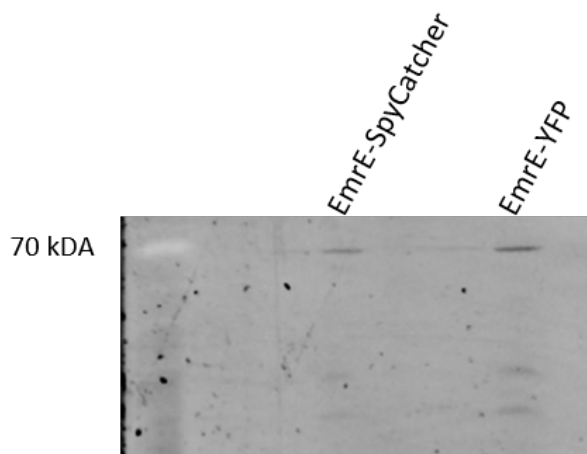


Figure 48: fluorescence image at 460 nm of 15 % SDS-PAGE with EmrE-SpyCatcher and -YFP membranes

5. Discussion

The goal of this thesis was to test different FRET-based sensors in order to quantify macromolecular crowding on the lipid membrane interfaces. For this, liposomes and Nanodiscs were used. By adding crowding agents to the synthetic membrane, simulation of a highly crowded surface could be achieved. With a proper sensor, this measurement system could be transferred to living cells to probe the phenomenon of macromolecular crowding.

Expression of all FRET sensor haven been successful. The synthesis of GFP-type fluorescent proteins takes several stages of processing, including folding, cyclization, dehydration, and aerial oxidation [14]. An overnight expression was chosen to provide enough time for those steps of protein maturation. This leads to a more equal amount of CFP and YFP in the FRET sensors providing more viable data [14]. In figure 9, 10, 11 the purified protein is visible with more than one band. This might appear due to conformational differences caused by the flexibility of the sensor. FRET 107 and 148 expressed in TB-medium showed viable absorbance spectra (figure 12). FRET 155 expressed in LB-medium indicated a higher fluorescence intensity than expressed in TB-medium (figure 16). Therefore, LB-media might be a better environment for fluorophore maturation.

SecE-SpyCatcher was successfully expressed and purified to serve as a membrane anchor domain (figure 18). Only SecE-SpyCatcher-126B variant was used for measurement because it has the shortest gap between the membrane and SpyCatcher enabling FRET sensors to bind closer to the synthetic membranes.

Measurements with the FRET sensors have shown different results due to different designs. FRET 107 was the most flexible sensor with only a connecting linker. FRET 148 and 155 were further modified with alpha helices and shorter linker, stabilizing the construct. The alpha helices also have a repulsive effect to each other which lead to smaller YFP/CFP ratio without crowding. Previous studies have shown that sensor without alpha helices have higher YFP/CFP ratios [15]. In agreement, FRET 107 variant shows a high YFP/CFP ratio already before introducing it into a crowded environment. Also, in the presence of crowding agents, FRET 107 showed the highest FRET signal due to its more flexible conformation (figure 22). The other sensors showed similar signals. Still, FRET 148 was affected the most by PEG4000 with a signal increase of 20% in 40 % PEG4000. Up to a concentration of 20 %, both PEG and Ficoll showed

comparable effects on the sensors. At elevated concentrations, PEG4000 resulted in a higher change in YFP/CFP ratio. This might be caused due to Ficoll being a compressible polymer which is likely to change shape at higher concentrations [16]. Binding FRET sensors to SpyCatcher has shown no difference in the signal without crowding for FRET 148 and 155. Surprisingly, FRET 107 had a decrease of 18 % in FRET signal (figure 23B).

When introducing the sensors to liposomes with SecE-SpyCatcher several challenges were faced. FRET sensors were able to bind the SpyCatcher but separating the bound complex from unbound FRET sensors was our greatest problem. For separation a multimodal chromatography (Capto Core 400) was tested. With this, larger molecules like viruses or proteoliposomes should elute, while soluble proteins should have bound to the column. In our observations (figure 25, 26), FRET sensor in its unbound state eluted together with proteoliposomes concluding the separation was not efficient. When using SEC with agarose-based columns for separation, a substantial loss of proteoliposomes could be observed. This might have been caused by the column filter, which affected the liposomes negatively e.g. retain or deform proteoliposomes, and the effect was specific to the liposome composition. DOPE proteoliposomes showed little to no elution of the bound FRET sensor, while PEG-containing samples indicated a faint band in the elution. PEG is an inert polymer which might have helped the liposomes to migrate through the column. However, when measuring emission spectra for those samples, it was concluded that PEG did not influence the FRET signal.

Another test without using SEC has shown the gradual binding of FRET after each hour (figure 31). In this test FRET sensors were added in a low amount to proteoliposomes with the intention to avoid SEC by binding every FRET sensor molecule to SpyCatcher on the liposomes. Binding FRET 107 to PEG-proteoliposomes proved problematic. This might be due to the excluded space caused by PEG molecules that form a cushion and hinder the sensor to reach the membrane. For DOPE- and biotin-proteoliposomes a complete binding of free FRET could not be achieved (figure 33). This leads to the assumption that more of SecE-SpyCatcher is not accessible for the sensor than we expected. We expected that 50 % of SpyCatcher might show inwards and cannot bind FRET sensors. For this reason, we decreased the molar ratio of FRET sensor to SecE-SpyCatcher even more to enable a complete binding of FRET sensors. Still, unbound FRET 107 could be found in the solution.

In another experiment, FRET sensors were bound beforehand to SecE-SpyCatcher and then reconstituted into liposomes to avoid the loading of proteoliposomes on SEC column. Figure 35 and 36 showed that PEG-proteoliposomes increased the YFP/CFP ratio as expected. In FRET 155 this ratio was decreased for only PEG-proteoliposomes which was the only sample without different conformations (figure 37). All biotinylated proteoliposomes covered with A1D3 showed the lowest FRET signal. Samples for this test showed high different bands in the fluorescence image. For this reason, an assumption whether the measured signal is caused by bound FRET sensor or not can't be made.

In a last experiment, Nanodiscs were used which ought to be more stable. After SEC, strong bands with bound FRET could be found in the elution separated from free FRET. Emission spectra for FRET 107 bound to different Nanodiscs have shown a decrease of CFP signal for PEG and DOPE. This was expected for PEG due to its crowding effect, but not for DOPE. With this, the higher FRET ratio could not be attributed to macromolecular crowding. Similar changes can be observed with FRET 155 where the overall energy transfer was low but with DOPE and PEG, the YFP signal rose higher. In FRET 148 no changes could be detected. Nanodiscs may allow SecE to move to the edge of the bilayer due to crowding. With this, the FRET sensors bound to SpyCatcher might be pushed away rather than compressed.

Due to decreased FRET ratios with biotinylated Nanodiscs and the addition of crowder A1D3 a test was performed to analyze A1D3 as a crowder. The test in figure 43 showed a successful binding of A1D3 to Nanodiscs in different amounts, but no difference in emission for FRET 107 could be detected (figure 44). It might be that FRET 107 isn't sensitive enough to detect the proteinaceous crowding induced by A1D3.

To probe SecE as a membrane protein for those tests, formed complexes of FRET sensor and E-SC were integrated into liposomes with thicker bilayers. By using thicker bilayers, SecE could be integrated completely without an overhanging part. Here FRET 148 and 155 showed no difference in PEG- and DOPE proteoliposomes (figure 45). Testing FRET 107 was not possible due to limited time of the project.

Furthermore, EmrE-SpyCatcher and EmrE-YFP constructs were cloned to act as substitute for SecE. However, the protein could not be found in cell membranes, but might have been mistargeted into the cytoplasm.

5.1. Conclusion

Fully matured FRET sensors were successfully expressed and purified as well as SecE-SpyCatcher and MSP. In solution, all sensors showed an expected increase of YFP/CFP ratio when introduced into a crowded environment. Reconstitution of E-SC into liposomes and Nanodiscs worked out and designed sensors were able to bind to E-SC on the synthetic membranes. We tested different ways of separating free FRET from bound FRET while FRET sensors bound to E-SC beforehand showed the most promising way of separation. With these tests, a separation by agarose-based SEC could be excluded due to the loss of proteoliposomes. Furthermore, we concluded that FRET sensors aren't able to bind completely to E-SC and Nanodiscs can't simulate the interfacial macromolecular of living cells properly. Nevertheless, PEG5000 demonstrated an increase in FRET ratio for FRET 107 and 148.

As an outlook, the binding of FRET sensors to E-SC reconstituted into liposomes must be optimized either by providing a complete binding or improving the separation of free and bound FRET sensors. In addition, SecE-SpyCatcher must be probed to exclude the possibility that it might affect the FRET signal in a crowded environment. Only with this, viable data can be obtained to study effects of crowding on the cell membrane.

6. References

1. Murade, C.U. and G.T. Shubeita, *A Molecular Sensor Reveals Differences in Macromolecular Crowding between the Cytoplasm and Nucleoplasm*. ACS Sens, 2019. **4**(7): p. 1835-1843.
2. Kuznetsova, I.M., K.K. Turoverov, and V.N. Uversky, *What macromolecular crowding can do to a protein*. Int J Mol Sci, 2014. **15**(12): p. 23090-140.
3. Ellis, R.J., *Macromolecular crowding: obvious but underappreciated*. Trends Biochem Sci, 2001. **26**(10): p. 597-604.
4. Kuznetsova, I.M., et al., *Beyond the excluded volume effects: mechanistic complexity of the crowded milieu*. Molecules, 2015. **20**(1): p. 1377-409.
5. Gnutt, D., et al., *Excluded-volume effects in living cells*. Angew Chem Int Ed Engl, 2015. **54**(8): p. 2548-51.
6. Howarth, M. and A.Y. Ting, *Imaging proteins in live mammalian cells with biotin ligase and monovalent streptavidin*. Nat Protoc, 2008. **3**(3): p. 534-45.
7. Liu, B., et al., *Design and Properties of Genetically Encoded Probes for Sensing Macromolecular Crowding*. Biophys J, 2017. **112**(9): p. 1929-1939.
8. SDS-PAGE Gel. CSH protocols, 2015.
9. Keeble, A.H. and M. Howarth, *Insider information on successful covalent protein coupling with help from SpyBank*. Methods Enzymol, 2019. **617**: p. 443-461.
10. Torchilin, V.P., *Recent advances with liposomes as pharmaceutical carriers*. Nat Rev Drug Discov, 2005. **4**(2): p. 145-60.
11. Skar-Gislinge, N., et al., *Elliptical structure of phospholipid bilayer nanodiscs encapsulated by scaffold proteins: casting the roles of the lipids and the protein*. J Am Chem Soc, 2010. **132**(39): p. 13713-22.
12. Howarth, M., et al., *A monovalent streptavidin with a single femtomolar biotin binding site*. Nat Methods, 2006. **3**(4): p. 267-73.
13. Dinant, C., et al., *Fluorescence resonance energy transfer of GFP and YFP by spectral imaging and quantitative acceptor photobleaching*. J Microsc, 2008. **231**(Pt 1): p. 97-104.
14. Liu, B., et al., *Influence of Fluorescent Protein Maturation on FRET Measurements in Living Cells*. ACS Sens, 2018. **3**(9): p. 1735-1742.
15. Hofig, H., et al., *Genetically Encoded Forster Resonance Energy Transfer-Based Biosensors Studied on the Single-Molecule Level*. ACS Sens, 2018. **3**(8): p. 1462-1470.
16. Boersma, A.J., I.S. Zuhorn, and B. Poolman, *A sensor for quantification of macromolecular crowding in living cells*. Nat Methods, 2015. **12**(3): p. 227-9, 1 p following 229.

7. List of figures

| | |
|---|----|
| Figure 1: effect of molecular size to excluded volume [3]..... | 2 |
| Figure 2: (A) FRET sensor bound to SecE-SpyCatcher on the membrane without crowding (B) FRET sensor bound to SecE-SpyCatcher on the membrane covered with PEG5000 | 3 |
| Figure 3: different versions of FRET sensors and SecE-SpyCatcher..... | 19 |
| Figure 4: 15 % SDS-PAGE of lysed cells before induction and before cell harvesting for preparations 1-7 of FRET 107. L= protein ladder, I= sample before Induction, H= before cell harvesting (A) fluorescence image at 460 nm of nonboiled samples (B) colorimetric image of Coomassie-stained boiled samples..... | 20 |
| Figure 5: 15% SDS-PAGE of IMAC purification of FRET 107. (A) fluorescence image at 460 nm (B) colorimetric image of Coomassie-stained unboiled samples. FT= flow-through, E= Elution. | 21 |
| Figure 6: (A) chromatogram of SEC for preparation 7 (B) colorimetric image of 15 % SDS-PAGE with Coomassie-stained SEC elution fractions | 21 |
| Figure 7: Absorbance spectrum for FRET 155 test (preparation 7)..... | 22 |
| Figure 8: Colorimetric image of 15 % SDS-PAGE with lysed cells before induction and before cell harvesting for FRET 107, 148, 155..... | 22 |
| Figure 9: (A) chromatogram of SEC for FRET 107 (B) colorimetric image of 15 % SDS-PAGE with Coomassie-stained Ni-NTA purification and SEC elution fractions of FRET 107 | 23 |
| Figure 10: (A) chromatogram of SEC for FRET 148 (B) colorimetric image of 15 % SDS-PAGE with Coomassie-stained Ni-NTA purification and SEC elution fractions of FRET 148 | 23 |
| Figure 11: Chromatogram of SEC for FRET 155 (B) colorimetric image of 15 % SDS-PAGE with Coomassie-stained Ni-NTA purification and SEC elution fractions of FRET 155..... | 24 |
| Figure 12: Absorbance spectrum for each FRET sensor of large-scale expression and purification (A)FRET 107 (B) FRET 148 (C) FRET 155..... | 24 |
| Figure 13: Fluorescence image of 15 % SDS-PAGE with lysed cells before induction and before cell harvesting for preparations for FRET 155 cultivated in LB- and TB-medium. I= sample before Induction, H= before cell harvesting..... | 25 |
| Figure 14: (A) chromatogram of SEC for FRET 155 (B) colorimetric image of 15 % SDS-PAGE with Coomassie-stained Ni-NTA purification and SEC elution fractions of FRET 155 in LB medium | 25 |
| Figure 15: (A) chromatogram of SEC for FRET 155 (B) colorimetric image of 15 % SDS-PAGE with Coomassie-stained Ni-NTA purification and SEC elution fractions of FRET 155 in TB-medium..... | 25 |
| Figure 16: Absorbance spectrum for FRET 155 expressed (A) in LB-medium (B) in TB-medium..... | 26 |
| Figure 17: Colorimetric image of 15 % SDS-PAGE with Coomassie-stained lysed cells before induction and before cell harvesting for preparations for E-SC-126, 126A, 126B. L= protein ladder, I= sample before Induction, H= before cell harvesting..... | 26 |
| Figure 18: Colorimetric image of 15 % SDS-PAGE with Coomassie-stained Ni-NTA purification and buffer exchange for E-SC-126, 126A, 126B..... | 27 |
| Figure 19: colorimetric image of Coomassie stained 15% SDS-PAGE with Coomassie-stained samples before induction with IPTG and cell harvesting and IMAC purification for MSP2N2, MSPE3D1 | 28 |
| Figure 20: Emission spectra for each sensor without crowding..... | 29 |
| Figure 21: Emission spectra for FRET 107 in PEG4000 with different concentrations | 29 |
| Figure 22: FRET ratio in PEG4000 and Ficoll FM70 with varying concentrations (A) for FRET 107 (B) for FRET 148 (C) for FRET 155 | 30 |
| Figure 23: (A) fluorescence image of 15 % SDS-PAGE with FRET 107, 148, 155 bound to SpyC (B) comparison of FRET ratios of free FRET and FRET bound to SpyC for FRET 107, 148, 155 without crowding agents | 31 |
| Figure 24: FRET ratio for FRET bound to SpyC in PEG4000 and Ficoll FM70 with varying concentrations A-C (A) FRET 107 (B) FRET 148 (C) FRET 155 | 32 |
| Figure 25: (A) chromatogram of multimodal chromatography for FRET 155 bound to DOPE-proteoliposomes (B) fluorescence image at 460 nm of 15 % SDS-PAGE with fractions took from the chromatography | 33 |
| Figure 26: (A) chromatogram of multimodal chromatography for FRET 155 bound to PEG-proteoliposomes (B) fluorescence image at 460 nm of 15 % SDS-PAGE with fractions took from the chromatography | 34 |

| | |
|---|----|
| <i>Figure 27: (A) chromatogram of SEC for DOPE- and PEG-proteoliposomes with FRET 107 (B) emission spectra of FRET 107 bound to proteoliposomes (C) colorimetric image of 15 % SDS-PAGE with samples from SEC for FRET 107 bound to proteoliposomes.....</i> | 35 |
| <i>Figure 28: (A) chromatogram of SEC for DOPE- and PEG-proteoliposomes with FRET 148 (B) emission spectra of FRET 148 bound to proteoliposomes (C) colorimetric image of 15 % SDS-PAGE with samples from SEC for FRET 148 bound to proteoliposomes.....</i> | 36 |
| <i>Figure 29: (A) chromatogram of SEC for DOPE- and PEG-proteoliposomes with FRET 155 (B) emission spectra of FRET 155 bound to proteoliposomes (C) colorimetric image of 15 % SDS-PAGE with samples from SEC for FRET 155 bound to proteoliposomes.....</i> | 37 |
| <i>figure 30 (A) chromatogram of SEC for DOPE -proteoliposomes with FRET 155 (B) colorimetric image of 15 % SDS-PAGE with samples from SEC for FRET 155 bound to 100 nm and 200 nm proteoliposomes</i> | 38 |
| <i>Figure 31: (A) fluorescence image at 460 nm of 15 % SDS-PAGE with samples picked each hour for PEG- and DOPE-proteoliposomes with FRET 107 (B) fluorescence image at 460 nm of 15 % SDS-PAGE with samples picked after 24 h for PEG- and DOPE-proteoliposomes with FRET 107 (C) band intensities for samples took each hour for PEG-proteoliposomes (D) band intensities for samples took each hour for DOPE-proteoliposomes</i> | 39 |
| <i>Figure 32: Emission spectra and YFP/CFP ratios for FRET 107 (A)(C) preparation with PEG-proteoliposomes (B)(D) preparation.....</i> | 40 |
| <i>Figure 33: Fluorescent image at 460 nm of 15 % SDS-PAGE with FRET 107, 148, 155 to DOPE- and biotin- proteoliposomes after 4 h incubation (A) first try (B) second try (C) third try</i> | 40 |
| <i>Figure 34: Chromatogram of SEC for FRET sensor bound to E-SC (A) FRET 107 (B) FRET 148 (C) FRET 155; Fluorescence image at 460 nm of elution fractions from SEC for FRET sensor bound to E-SC (D) FRET 107 (E) FRET 148, 155.....</i> | 41 |
| <i>Figure 35: fluorescence image at 460 nm for 15 % SDS-PAGE with starting material, supernatant and resuspended pellet of DOPE-, PEG-, Biotin-proteoliposomes bound with FRET sensor (A) FRET 107 (B) FRET 148 (C) FRET 155.....</i> | 42 |
| <i>Figure 36: (A) emissions spectra and (B) CFP/YFP ratio for FRET 107 bound to DOPE-, PEG and Biotin- proteoliposomes</i> | 43 |
| <i>Figure 37: (A) emissions spectra and (B) CFP/YFP ratio for FRET 148 bound to DOPE-, PEG and Biotin- proteoliposomes</i> | 43 |
| <i>Figure 38: (A) emissions spectra and (B) CFP/YFP ratio for FRET 155 bound to DOPE-, PEG and Biotin- proteoliposomes</i> | 43 |
| <i>Figure 39: Chromatograms of SEC for E3D1 DOPE-Nanodiscs in different sizes.....</i> | 44 |
| <i>Figure 40: (A) chromatogram for DOPE-, PEG- and Biotin-Nanodiscs with FRET 107 (B) fluorescence image of 15 % SDS-PAGE with sample after centrifugation and elution fractions after SEC for FRET 107 (C) emission spectra for FRET 107 and FRET 107 bound to DOPE-, PEG- and Biotin-Nanodiscs (D) YFP/CFP ratios for FRET 107</i> | 45 |
| <i>Figure 41: (A) chromatogram for DOPE-, PEG- and Biotin-Nanodiscs with FRET 148 (B) fluorescence image of 15 % SDS-PAGE with sample after centrifugation and elution fractions after SEC for FRET 148 (C) emission spectra for FRET 148 and FRET 148 bound to DOPE-, PEG- and Biotin-Nanodiscs (D) YFP/CFP ratios for FRET 148</i> | 46 |
| <i>Figure 42: (A) chromatogram for DOPE-, PEG- and Biotin-Nanodiscs with FRET 155 (B) fluorescence image of 15 % SDS-PAGE with sample after centrifugation and elution fractions after SEC for FRET 155 (C) emission spectra for FRET 155 and FRET 155 bound to DOPE-, PEG- and Biotin-Nanodiscs (D) YFP/CFP ratios for FRET 155</i> | 47 |
| <i>Figure 43: (A) chromatograms of SEC for FRET 107 and A1D3 bound to Nanodiscs with different amounts of Biotin; 15 % SDS-PAGE with elution fractions from SEC (B) fluorescence image at 460 nm (B) colorimetric image of Coomassie-stained samples</i> | 48 |
| <i>Figure 44: Emission spectra for FRET 107 bound to Nanodiscs with different amounts of Biotin</i> | 48 |
| <i>Figure 45: (A) fluorescence image at 460 nm of SDS-PAGE with FRET 148 and 155 bound to DOPE- and PEG- proteoliposomes; Emission spectra for FRET sensors bound to DOPE- and PEG proteoliposomes (B) FRET 148 (C) FRET 155;.....</i> | 49 |
| <i>Figure 46: (A) colorimetric image of 15 % SDS-PAGE with Coomassie-stained samples from Ni-NTA purification washed with 10 mM, 20 mM, 30 mM imidazole (B) fluorescence image at 460 nm of EmrE-SpyCatcher+FRET 107 binding.....</i> | 50 |
| <i>Figure 47: Fluorescence image at 460 nm of 15 % gel with EmrE-YFP cells lysed by B-PER</i> | 51 |
| <i>Figure 48: fluorescence image at 460 nm of 15 % SDS-PAGE with EmrE-SpyCatcher and -YFP membranes</i> | 51 |

8. List of tables

| | |
|--|-----------|
| <i>Table 1: FRET sensor and SecE-SpyCatcher constructs used in this thesis</i> | <i>6</i> |
| <i>Table 2: PCR settings for first step of EmrE insert preparation</i> | <i>13</i> |
| <i>Table 3: PCR settings for second step of EmrE insert preparation</i> | <i>13</i> |
| <i>Table 4: PCR setting for SpyCatcher vector preparation.....</i> | <i>14</i> |
| <i>Table 5: Composition of preparations for Gibson-Assembly</i> | <i>14</i> |
| <i>Table 6: Lipid composition of liposomes used in this thesis</i> | <i>16</i> |

9. List of abbreviations

| abbreviation | Chemical |
|--------------|---------------------------------------|
| amp | Ampicillin |
| EDTA | Ethylenediaminetetraacetic acid |
| HCl | Hydrogen chloride |
| IPTG | Isopropyl-β-D-1-thiogalactopyranoside |
| kam | Kanamycin |
| DDM | n-Dodecyl β-maltoside |
| KOAc | Potassium acetate |
| PMSF | Phenylmethylsulfonylfluoride |
| NaCl | Sodium chloride |
| NaOH | Sodium hydroxide |
| TCEP | Tris(2-carboxyethyl) phosphine |
| TRIS | Tris(hydroxymethyl)aminomethane |